September 10, 2013
Volume 46
Number 17

Macromolecules

pubs.acs.org/Macromolecules

Reactive Polyolefin Approach for Preparing Functional Polyolefins for Energy Applications

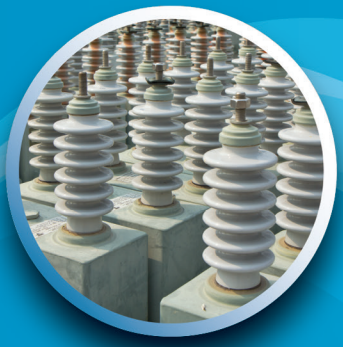

High Energy & Power Density Capacitors

Ion-Conducting Membranes for Electrochemical Devices

Oil-Superabsorbent for Oil Spill Recovery

ACS Publications
MOST TRUSTED. MOST CITED. MOST READ.

www.acs.org

Macromolecules

Perspective

pubs.acs.org/Macromolecules

Functional Polyolefins for Energy Applications

T. C. Mike Chung*

Department of Materials Science and Engineering, The Pennsylvania State University, University Park, Pennsylvania 16802, United States

ABSTRACT: Polyolefins, including polyethylene (PE) and polypropylene (PP), represent more than half of commercial polymers produced in the world. They are known to be cost-effective and good performing materials used in a broad range of commodity applications that influence our everyday lives. On the other hand, less attention has been paid to their specialty applications, commonly requiring the material to have multiple performance functions. The limitations and shortcomings of polyolefins have stemmed from lack of functionality and structure diversity, which are compounded with the long-standing challenges in the chemical modification (functionalization) of polyolefins. In the past two decades, in conjunction with advances in metallocene catalysis, a new method based on the "reactive" polyolefin approach has emerged, which affords a new class of functional polyolefins with high molecular weight and well-controlled molecular structures that have functional groups located at chain ends, side chains, and block/graft segments. In addition to forming distinctive multiple phase morphology with shape hydrophobic−hydrophilic microphase separation and surface properties, some functional polyolefins with flexible polar (or ionic) groups offer excellent mobility for polarization, ion conductivity, etc. They present potentials for polyolefins in high-value, specialty applications. In this paper, I will cover three energy-related areas, including polymer film capacitors for electric energy storage, ion exchange membranes for hydrogen energy, and oil superabsorbent polymers for oil spill recovery, to discuss the effects of new polyolefin structures on their performances and the future perspectives. The objective is to provide examples that reveal underlying benefits of this new class of high-performance, cost-effective functional polyolefin materials and hopefully inspire more researchers to explore their applications.

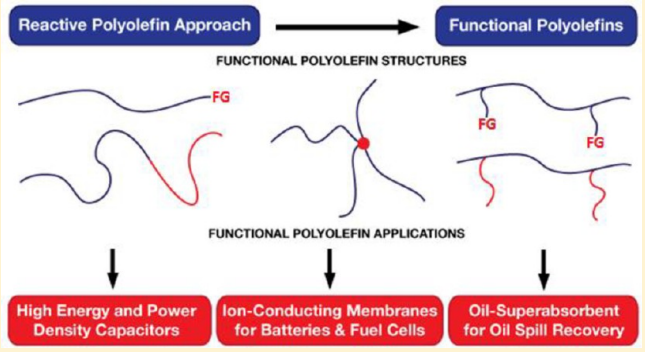

1. INTRODUCTION

Polyolefins, including polyethylene (PE) and polypropylene (PP) with the simplest polymer structures, represent more than half of commercial polymers produced in the world. They are mostly used in commodity applications that influence our day-to-day life, with a unique combination of chemical and physical properties, excellent processability and recyclability, and low cost. On the other hand, less attention has been paid to their contributions in specialty areas. In energy storage devices, the biaxially oriented polypropylene (BOPP) thin films are state-of-the-art dielectrics in capacitors, and the microporous polypropylene and polyethylene films are commonly used as the separators between the cathode and anode in Li-ion batteries. They offer cost-effective materials with several desirable polyolefin properties, including electric insulation and chemical, thermal, and mechanical stability. At the same time, however, they also exhibit some shortcomings, such as weak dielectric responses in the polymer dielectric film and lack of hydrophilicity in the separator, that limit their performance and wider acceptance in specialty, high-value applications. These applications usually require materials with mutiple performance functions and, at times, a specific morphology.

Since the Ziegler and Natta era in the 1950s,[1−3] an importance grew to modify and functionalize polyolefins to improve their interactive properties, especially in the areas of coating, blends, and composites, in which adhesion, comparability, and paintability are paramount. The perpetual interest in the past six decades has been driven by an impetus to improve polyolefin properties for higher-value products. However, chemical modification and functionalization of polyolefins these days, to a large extent, still remain a scientifically challenging and industrially important research area. There are thousands of reports and patents that discuss the functionalization approaches involving both direct and postpolymerization processes with limited industrial success. As will be discussed, some fundamental issues in heterogeneous Ziegler−Natta cayalysts (direct process) and stable polyolefin chemical structures (postprocess) have posted huge technological barriers for finding an acceptable chemical route to prepare large-scale functional polyolefins.

In the early 1980s, the discovery of homogeneous metallocene catalysts[4−8] provided a new era in the polyolefin industry as well as a new opportunity to develop novel polyolefin structures. In addition to their superior catalytic

Received: June 16, 2013
Revised: August 1, 2013
Published: August 13, 2013

 © 2013 American Chemical Society dx.doi.org/10.1021/ma401244t | *Macromolecules* 2013, 46, 6671−6698

activities, the major advantage of the metallocene catalyst is its single, well-defined, and tunable (by ligands) active site and the associated, well-controlled reaction mechanism. Several PE and PP copolymers containing large comonomers, including styrenic and cyclic ones, were effectively prepared with high molecular weight, a broad range of copolymer compositions, and narrow molecular weight and composition distributions. It was apparent to us that it might be possible to design new comonomers and chain transfer agents, in conjunction with some selected metallocene catalysts, to prepare new polyolefin copolymers or chain end-capped polyolefins. Since the late 1980s, our research group (initially at Exxon Corporate Research and then at Penn State University) has been investigating the means of applying this new metallocene technology into our new functionalization scheme (so-called "reactive" polyolefin approach)[9−12] to circumvent the chemical difficulties in direct and postpolymerization processes and studying the properties and applications of functional polyolefins. As will be discussed, several "reactive" comonomers and chain transfer agents have been discovered and can be effectively incorporated into polyolefin structures. In addition, the incorporated "reactive" groups can be selectively interconverted to polar functional groups or, preferably, be transformed to initiators for graft-from polymerization of functional monomers to prepare new polyolefin graft/block copolymers.

In the dawn of this century, the rapid, industrial development in China and some developing countries has significantly increased the global consumption of fossil fuels, including feedstocks for producing polyolefin materials. The control of oil resources has, in large part, been an underlying cause of political conflict and warfare. The deteriorating environment, ecosystems, and global warming, due to the exploration, transport, and use of fossil energy resources, have been threatening our civilization and posting uncertainty to future generations. It is urgent that innovators develop new energy technology that can provide efficient, safe, environmentally friendly, and economical extraction, conversion, transportation, storage, and use of energy. There are several clean and renewable energy technologies under various stages of development and commercialization. However, oftentimes, the lack of suitable material to provide a specific combination of strong properties and performance functions has limited technologies from achieving their full potential and from seeing large-scale applications. In this paper, we will discuss three energy-related areas polymer film capacitors for electric energy storage, ion exchange membranes for fuel cells and other electrochemical devices, and oil superabsorbent polymer for oil spill recovery, with which we designed and synthesized new polyolefin materials and showed some interesting results.

2. CHALLENGES IN ENERGY TECHNOLOGY

2.1. Energy Storage Technologies. Energy storage has long been a scientifically challenging and industrially important area and is essential to energy utilization and management. If an energy storage technology could provide similar energy and power densities as the combustion engines and gas turbines that are available today (Figure 1), we might very well rectify many of our energy and environmental problems. There are several advantageous scenarios that effective energy storage may offer: high performance electric vehicles could become a reality; clean solar and wind energy generated at peak hours could be used throughout down time; and the energy generation system could be designed based on the average usage capacity instead of the peak consumption level. Although many energy storage devices, namely fuel cells, batteries, electrochemical supercapacitors, and conventional capacitors, are commercially available and their storage mechanisms have been well-known for decades, they are relatively expensive and can only be used in special applications. They also perform significantly lower than prevalent combustion systems in energy density and/or power density. Among them, fuel cells, batteries, and supercapacitors, based on electrochemical energy, are limited by electrochemical potential and stability of electrolytes, resulting in low cell voltage and low power density. On the other hand, conventional capacitors can offer very high power density but only very low energy density in current devices (Figure 1).

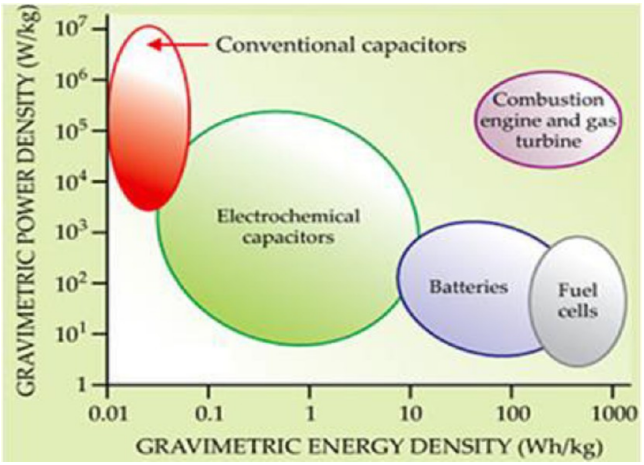

Figure 1. Energy and power densities of various energy storage methods.

2.2. Polymer Film Capacitors. Capacitors[13−15] are passive electronic devices that store energy electrostatically. In their simplest form, capacitors consist of two conducting plates (positive and negative electrodes) separated by an insulating material called the dielectric, which can be air, ceramics, polymers, etc. Contrary to batteries, which have high energy density and low power density, capacitors usually exhibit high power density but very low energy density. The inherent, scientific challenge is to increase the energy density of the capacitor, which is governed by the dielectric that separates the opposite static charges on two electrode surfaces. Recently, the metallized polymer film capacitors[16,17] have attracted a great deal of attention due to their desirable properties, such as light weight, low cost, and excellent processability for forming thin film with a large surface area. They also demonstrate flexibility and toughness under stress and the ability to be packaged into a desirable configuration. Currently, state-of-the-art polymer film capacitors are based on BOPP thin films.[18,19] Despite the low energy density, ~2 J/cm^3, BOPP shows almost no energy loss during the charging−discharging cycles and self-healing after a film puncture, which merely results in a gradual loss of capacitance, and thus can be operated close to the breakdown voltage with long-term reliability. Many BOPP capacitors are currently used as pulse power conditions in commercial and military devices. On the basis of the energy density equation (discussed later), it is theoretically possible to increase the energy density of capacitors by increasing the polymer dielectric constant (ε) and/or the applied electric field (E)

dx.doi.org/10.1021/ma401244t | Macromolecules 2013, 46, 6671−6698

that is limited by breakdown strength. So far, there has been limited research activity around polymer film dielectrics. The major challenge is about how we can develop a new polymer dielectric with a combination of properties, including a high dielectric constant, low loss, high breakdown strength, good mechanical and thermal stability, and cost-effectiveness. As will be discussed, our recent experimental results, using two designed functional PP polymers, interestingly showed the increase of both the dielectric constant and breakdown strength without altering other desirable PP properties.

2.3. Separators and Ion Conductors. Another polyolefin material used in energy storage application includes microporous PE and PP membranes that are commonly used as separators[20,21] between anode and cathode electrodes, which are critical components in batteries. The ideal separator would be infinitesimally thin, offer no resistance to ionic transport in electrolytes, provide infinite resistance to electronic conductivity for isolation of electrodes, be highly tortuous to prevent Li dendritic growths and separator punctures (in Li-ion batteries), and be inert to chemical reactions. Unfortunately, in the real world, an example of this ideal does not exist; their ionic conductivity is brought to the desired range by manipulating the membranes' thickness and porosity. In addition, hydrophobic polyolefin separators are prone to fouling that gradually reduces the device capacity and performance. There is no single separator that satisfies all needs of battery designers, and compromises have to be made. On the other hand, there has been a continued demand for thinner battery separators to increase battery power and capacity. This has been especially true for portable electronics, automotive, and aviation applications. In many cases, the separator is the major limiting factor for life and performance of batteries. In researching for the next generation of batteries with increased reliability and performance, it is interesting to investigate new hydrophilic polyolefin films that could prevent separator fouling, puncturing, and beyond. Preferably, the functionality of the polymer film could be further extended to include ion conductivity. In other words, the challenge is to develop new solid polymer electrolytes (SPEs) and ion conductive membranes (IEMs) that can provide both a separator function (electric insulator) and high ion conductivity (and selectivity) at ambient temperatures. Without an organic solvent, the Li ion battery would dramatically increase in safety. Solid electrolytes with high ion conductivities are always desirable for all electrochemical devices. As will be discussed, we have designed and synthesized several polyethylene-based ion-containing membranes, having the ion moieties located at the end of flexible side chains and/or hydrophilic channels, which show interesting ion conductivity at ambient conditions.

2.4. Oil Spills and Enviornmental Impacts. Despite the push for clean and renewable energy resources, we will seemingly still need fossil fuels for energy and chemical resources for decades to come. In light of the 2010 BP oil spill in the Gulf of Mexico, we still have no effective technology for removing, recovering, and cleaning up oil spills or oil slicks from the surface of seawater and shorelines. Despite the government's "all hands on deck" approach to combating the oil spill, current methods of booms and skimmers, dispersants, and *in situ* burning are decades-old and manpower-intensive technologies. Applying massive amounts of the chemical dispersant Corexit helped to break up the surface oil but raised questions about the safety of the product and long-term environmental impacts. The unknown environmental consequences are dependent on its toxicity and biodegradability that may vary from one location to another. On the other hand, booms and skimmers cannot prevent the evaporation of lighter or more volatile hydrocarbons within the oil mixture, nor prevent emulsification of small oil–water droplets to hamper the recovery and cleanup process. Their efficiencies are highly dependent on weather conditions. While most booms perform well in gentle seas, the forces exerted by currents, waves, and wind may impair the ability of a boom to hold oil. In choppy water, skimmers tend to recover more water than oil. Only a small percentage of spilled oil was actually recovered in the BP oil spill by booms and skimmers, and they generated a large quantity of solid and liquid waste from soiled booms and other oily waste that may eventually become secondary pollution. Based on these methods, most spilled oil is wasted and ultimately becomes pollutants in our air and water.

When an oil spill occurs on water, the first few hours of action are crucial in determining the effectiveness of later recovery, removal, and disposal as well as the level of environmental impact. To minimize the danger to people and property, the immediate protocol shall restrict the initial spread of oil and the evaporation of light hydrocarbons into the air. The application of suitable oil sorption materials is an attractive approach. If they could be precisely and quickly applied by low-flying airplanes or helicopters under most weather conditions, even in remote locations, they might immediately stabilize the spilled oil as well as help in the actual removal of spilled oil. The economic and environmental concerns surrounding oil spills encouraged many researchers to investigate natural sorption materials, such as multifarious inorganic porous products (i.e., clay, talc, zeolites, silica aerogel, calcium fly ash, etc.)[22,23] and organic biodegradable products (straw, hull, corncob, peat moss, sugar cane bagasse, wood/cotton fibers, wool-based materials, silkworm cocoon waste, etc.).[24−30] However, most of them show limited oil sorption capacity and also absorb water, thus making recovered solids unsuitable for calcinations; most of them end up in landfills. Currently, meltblown PP (fiber-based) pads and booms[31,32] are the most commonly used oil sorbent materials. They are frequently used to remove final traces of oil or used in areas that cannot be reached by skimmers. They are also common in machine shops and oil storage facilities to clean up small oil leaks. After recovering the oil, however, they are often disposed. They adsorb oil in their interstices via capillary action (*adsorption mechanism*), with the adsorption capacity proportional to the surface area. Because of the weak oil–substrate interaction, the fiber-based adsorbers exhibit many disadvantages, including low adsorption capacity, failure to maintain oil of low viscosity, and easy rebleeding of adsorbed oil under a slight external force. Recently, several papers applied the high surface area materials, including nanowire membranes,[33] nanocellulose aerogels,[34] and carbon nanotubes,[35] to increase oil adsorption capacity. In addition to the cost, treatment of recovered solid materials is a major concern, including waste disposal, recyclability, and biodegradability. Overall, it is a major scientific challenge to develop a suitable oil sorption material that further addresses the treatment of recovered solid wastes.

3. SYNTHESIS OF FUNCTIONAL POLYOLEFINS

As discussed, the limitations and shortcomings of polyolefins have stemmed from the lack of functionality and structure diversity, which have been compounded with the long-standing challenges in the chemical modification (functionalization) of

polyolefins. Generally speaking, there are three research approaches to tackle the functionalization challenge in polyolefins. As illustrated in Scheme 1, they include (a) direct

Scheme 1. Three Functionalization Approaches

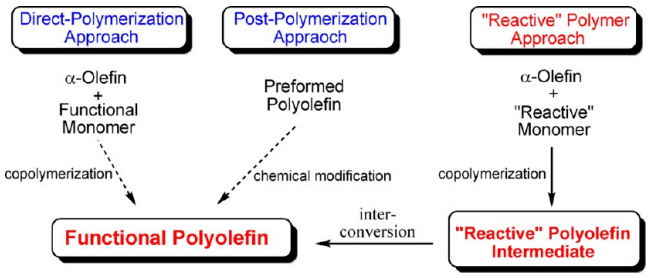

copolymerization of α-olefin with a functional monomer, (b) chemical modification of the preformed polyolefin, and (c) a reactive polymer intermediate that can be effectively prepared and then selectively interconverted to functional groups under mild reaction conditions.

The first two approaches are more obvious and naturally have enjoyed the most attention. In the past, they were referred to as direct and postpolymerization processes, respectively. The third approach is relatively new and one mostly developed in our laboratory. This approach has benefited greatly from metallocene technology, especially due to its well-defined reaction mechanism and superior capability in copolymerization and chain transfer reactions. As will be discussed, the new approach has opened up the opportunity to design new reactive comonomers and chain transfer agents, resulting in a broad range of new functional polyolefin with compositions and structures that would be very difficult to prepare by other methods. The following sections will discuss the scope and limitations of each process. The chemical reasoning may provide a general perspective of each functionalization approach.

3.1. Direct-Polymerization Approaches. The direct-polymerization process[36−52] could be an ideal if the copolymerization of ethylene or propylene with functional monomers was as effective and straightforward as the corresponding homopolymerization. Unfortunately, some fundamental chemical difficulties, namely catalyst poisoning and some side reactions (such as chain walking, chain transfer reactions, and various coordination−insertion mechanisms), are difficult to entirely control; copolymerization reactions cannot achieve the ideal functional HDPE and i-PP polymers with desirable copolymer structures and properties. The small number of catalytic (cationic) sites tends to form complexes with nonbonded electron pairs on N, O, and X (halides) of functional monomers, preferring to react with the π-electrons of the double bonds. The result is the deactivation (or retardation) of the active polymerization sites due to side reactions or the forming of stable complexes between catalysts and functional groups, via both inter- or intramolecular mechanisms, thus inhibiting polymerization to achieve high polymers. Two general approaches include (i) protecting the sensitive functional group from the poisoning catalyst by introducing bulky alkyl or silane groups or by precomplexing the functional group with aluminum alkyl compound employed in the catalyst preparation[36−45] or (ii) employing late transition metal catalysts that are less oxophilic and more stable to heteroatoms.[46−52] So far, most experimental results show a significant decrease in catalyst activity and polymer molecular weight, forming a branched PE chain in late transition metal catalyst cases, which reduces polymer crystallinity and melting temperature.[49−51] Some research efforts[53−57] were dedicated to applying high ethylene pressure and appropriate late transition metal complexes to suppress the chain walking process and form linear PE. However, most resulting functional PE copolymers are low molecular weight materials. In addition, it would be a challenge to extend this late transition metal approach to prepare functional isotactic polypropylene polymers. Despite perpetuating interest, the combination of chemistry difficulties has prevented serious consideration of the direct process for commercial applications.

3.2. Postpolymerization Approaches. Current commercial functionalization methods are based on the postpolymerization process.[58,59] Chemical modifications of the preformed polyolefins have been usually carried out *in situ* during the fabrication process to reduce production cost as well as to relieve concerns surrounding the reduction of the processability of polyolefins after the functionalization reaction. However, the combination of the inert nature of the polyolefin and a short reaction time (during processing) causes great difficulty in controlling the polymer composition and structure. There is no facile reaction site in the saturated HDPE and PP polymer chains. The only successful tactic is to use a free radical initiator or radiation to activate the polymer by breaking some stable C−H bonds and forming free radicals along the polymer chain for free-radical grafting reactions. Scheme 2 illustrates the

Scheme 2. Reaction Mechanism for the Free Radical Mediated Grafting Reaction on PP

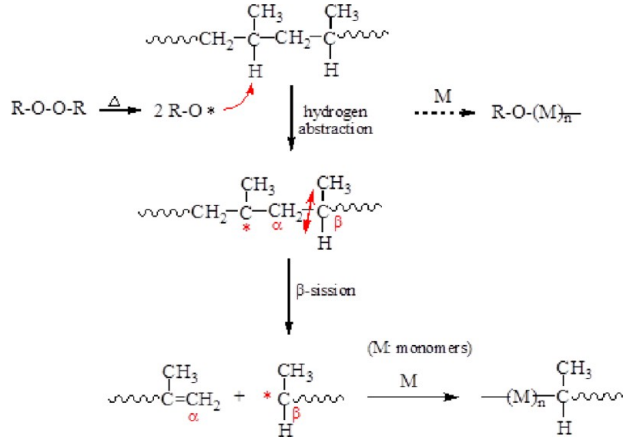

general reaction mechanism, including the formation of maleic anhydride modified polypropylene (PP-MAH)[60] which is the most crucial commercial functionalized PP polymer. It is commonly used to improve PP's poor interactive properties[61−63] and broaden its applications to higher value blends and composites—those in which adhesion and compatibility with other materials are paramount.

After hydrogen abstraction of tertiary protons in PP chain by free radicals, the formed tertiary macroradicals in the PP chain immediately involve a facile intramolecular β-scission reaction and degrade the polymer chain into two shorter PP chains:[64−70] one with an unsaturated chain end and the other having a terminal macroradical that subsequently reacts with maleic anhydride monomers. As expected, the incorporated MAH content is inversely proportional to PP molecular weight.

dx.doi.org/10.1021/ma401244t | Macromolecules 2013, 46, 6671−6698

Many experimental results also suggest that the incorporated MAH monomer units are a mixture of single and multiple succinic anhydride moieties due to the oligomerization of maleic anhydride. In addition, other side reactions, such as the direct oligomerization of MAH monomers by the alkoxyl radical to form the ungrafted impurities, also take place during this free radical grafting reaction, especially under high reaction temperatures. The final product is usually a complicated, deep-colored mixture. Unfortunately, the performance of PP−MAH as an interfacial agent is highly dependent on its molecular weight and MAH content as well as the ability to remove impurities.

3.3. "Reactive" Polymer Approach. In the early 1980s, the discovery of homogeneous metallocene catalysts[4−8] provided an excellent opportunity for exploring new functionalization approaches to circumvent the chemical difficulties in direct and postpolymerization processes. Comparing with heterogeneous (multiple active sites) Ziegler−Natta catalysts, one major advantage of the homogeneous (single-site) metallocene catalyst is its superior capability in the copolymerization reaction to form copolymers with high molecular weight and narrow molecular weight and composition distributions. The tunable active site (controlled by ligands) allows for the effective incorporation of large comonomers into PE and PP copolymers with a broad range of copolymer compositions. In the late 1980s, we were contemplating about how we could apply this new metallocene-mediated copolymerization capability into our functionalization chemistry and study the properties and applications of the resulting functional polyolefins.[9−12] Scheme 3 illustrates our general strategy, now called the "reactive" polyolefin approach.[71−75]

Scheme 3. Reaction Route Using Reactive Comonomers To Prepare Functional Polyolefins and Polyolefin Graft Copolymers

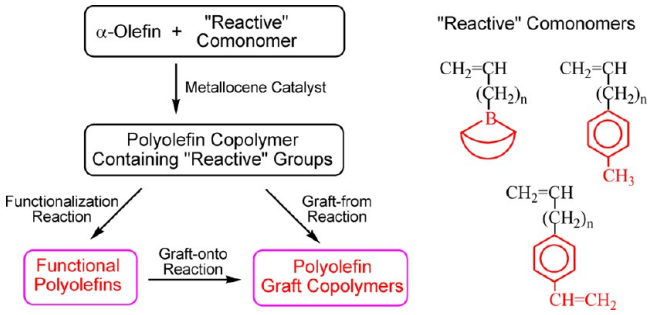

The design of the comonomer containing a "reactive" group that shall exhibit three essential properties, including (i) good stability with metallocene catalyst, (ii) good solubility with the reaction media, and (iii) facile interconversion of the reactive group into functional (polar) groups after polymerization.[4] In the past two decades, we had identified three suitable "reactive" groups, including organoborane, benzylic protons (φ-CH_3), and styrene moieties. In concert with the selected metallocene catalysts, the copolymerization reactions take place to form well-controlled "reactive" polyolefin copolymers with a designed amount of "reactive" sites in the side chains. Subsequently, they can be effectively interconverted into functional polyolefin containing functional groups (such as OH, NH_2, etc.) under mild reaction conditions. More interestingly, they are transformed into a "living" radical or anionic initiator to initiate a graft-from polymerization to form polyolefin graft copolymers[71,76,77] with a polyolefin (PE, PP, etc.) backbone and several functional polymer (acrylate, methacrylate, etc.) side chains. As will be discussed later, some reactive groups in the copolymer serve as cross-linkers in forming PE and PP networks, and the resulting functional polyolefins also involve coupling (graft-onto) reactions with polycondensation polymers to form graft copolymers.[78,79]

As illustrated in Scheme 4, the first one is a borane-containing comonomer that contains a α-olefin moiety for copolymerization and a "reactive" borane group for the functionalization reaction. The initial decision to choose the borane moiety was based on the unique location of boron (B) in the periodic table, which is the only nonmetallic and electron-deficient element. The Lewis acidic nature of borane offers itself a very good chance of coexisting with transition metals (Lewis acids). In addition, the size of the boron atom is relatively small, and steric protection can be effectively applied if needed. Therefore, a α-olefin containing borane group shall be able to be incorporated into the polymer using metallocene catalysis. Boron is situated next to carbon in the periodic table. Both elements are similar in atomic size, and the B−C bond is covalent in nature. The borane-containing polymers will behave like regular hydrocarbon polymers with similar solution properties, such as solubility and viscosity. Therefore, the same reaction conditions and processes for α-olefin polymerization can be directly applied to its copolymerization reaction with a borane monomer. High molecular weight and high yield of borane containing polymers are expected. On the other hand, the incorporated borane groups can be effectively transformed to a remarkably fruitful variety of functionalities under mild reaction conditions, as shown by Professor Brown.[80] In addition, the borane groups can be transformed to the macroinitiators for forming the polyolefin graft copolymer, which will be discussed later.

Table 1 compares the copolymerization results[81−83] between α-olefin (ethylene, propylene, and 1-octene) and 5-hexenyl-9-BBN (9-BBN: 9-borabicyclo[3.3.1]nonane) using two important homogeneous metallocene catalysts, including [(η^5-C_5Me_4)$SiMe_2$-(η^1-$NCMe_3$)]$TiCl_2$ (CGC; constrained geometry catalyst) for ethylene and *rac*-Me_2Si[2-Me-4-Ph-(Ind)]$_2ZrCl_2$ for propylene, and the heterogeneous $TiCl_3$·AA/Et_2AlCl Ziegler−Natta catalyst for both ethylene and propylene copolymerization reactions. Comparing runs A-1 to A-4 (using CGC catalyst), the concentration of borane groups in polyethylene is basically proportional to the concentration of the borane monomer feed. It is unexpected that the catalyst activity systematically increases with the concentration of the borane monomer. Evidently, no retardation due to the borane groups is shown in these cases. This CGC catalyst, with an open active site for accommodating a relatively large borane monomer, shows satisfactory copolymerization results at 150 °C, similar to those in the preparation of linear low density polyethylene (LLDPE). On the other hand, the heterogeneous $TiCl_3$·AA/Et_2AlCl catalyst (runs B-1 and B-2, with a high concentration of the borane comonomer) shows no detectable borane group in the copolymer.

The same functionalization route was extended to higher α-olefin copolymers. Both isospecific metallocene and heterogeneous Ziegler−Natta catalysts (sets C and D) were employed in propylene copolymerization reactions with 5-hexenyl-9-BBN. With the general phenomenon in the Ziegler−Natta mediated copolymerization, the bigger the size of the monomer, the

dx.doi.org/10.1021/ma401244t | *Macromolecules* 2013, 46, 6671−6698

Scheme 4. "Reactive" Borane Comonomer Approach To Prepare Functional Polyolefins

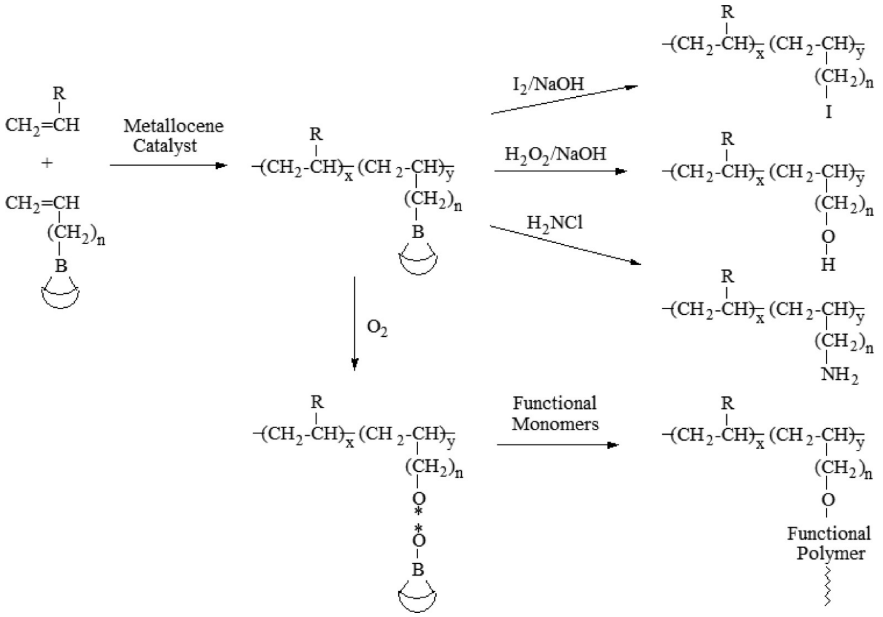

Table 1. Copolymerization Reactions between α-Olefin (M_1) and 5-Hexenyl-9-BBN (M_2) and the Resulting Hydroxylated Polymers

		polymerization conditions				hydroxylated polymer products			
run	catalyst[a]	α-olefin[b] (psi or g)	comonomer[c] (mol %)	temp (°C)	time (min)	comonomer[d] (mol %)	M_w (kg/mol)	T_m (°C)	ΔH (J/g)
A-1	**1**	C_2/450 psi	0	150	5	0	105	133.8	244
A-2	**1**	C_2/450 psi	10	150	5	1.46	85	123.2	195
A-3	**1**	C_2/450 psi	20	150	5	2.75	76	110.3	152
A-4	**1**	C_2/450 psi	30	150	5	4.65	55	103.4	138
B-1	**3**	C_2/450 psi	20	60	110	0		133.5	242
B-2	**3**	C_2/450 psi	30	60	110	0		133.3	238
C-1	**2**	C_3/120 psi	5	60	60	1.5	210	146.5	45.2
C-2	**2**	C_3/120 psi	10	60	60	3.2	175	133.7	32.5
C-3	**2**	C_3/120 psi	15	60	60	6.0	120	87.5	21.6
D-1	**3**	C_3/120 psi	10	70	60	0.7	490	156.7	66.1
D-2	**3**	C_3/120 psi	20	70	60	1.8	592	156.6	65.4
D-3	**3**	C_3/120 psi	40	70	60	4.2	392	156.2	65.2
E-1	**3**	C_8/10 g	25	30	90	15	1580		
E-2	**3**	C_8/7 g	50	30	90	40	1030		
E-3	**3**	C_8/4 g	75	30	90	65	280		

[a]Catalyst **1**: $[(\eta^5\text{-}C_5Me_4)SiMe_2\text{-}(\eta^1\text{-}NCMe_3)]TiCl_2$; catalyst **2**: *rac*-$Me_2Si[2\text{-Me-4-Ph(Ind)}]_2ZrCl_2$; catalyst **3**: $TiCl_3$·AA/Et_2AlCl. [b]C_2: ethylene, C_3: propylene, C_8: 1-octene. [c]Comonomer: 5-hexenyl-9-BBN. [d]Comonomer content (mol %) in the copolymer determined by the ^1H NMR spectrum. [e]Estimated by intrinsic viscosity.

lower the reactivity and the more easily it becomes to copolymerize the borane monomer with high α-olefins. Reactivity ratios were obtained at r_1 = 70.476, r_2 = 0.028, and $r_1 \times r_2$ = 1.973 for propylene/5-hexenyl-9-BBN[81] using the $TiCl_3$·AA/Et_2AlCl catalyst. The values of $r_1 \times r_2$ are far from unity. The copolymerization reaction between propylene and 5-hexenyl-9-BBN is favorable for propylene incorporation to form a taped copolymer microstructure. The same propylene/5-hexenyl-9-BBN copolymerization was also conducted using the *rac*-$Me_2Si[2\text{-Me-4-Ph(Ind)}]_2ZrCl_2$/MAO catalyst. The results show reactivity ratios of propylene at r_1 = 1.782 and 5-hexenyl-9-BBN r_2 = 0.461. The value of $r_1 \times r_2$ = 0.821 is close to unity, indicating a relatively good random copolymerization reaction. The copolymers show high molecular weight and narrow molecular weight distribution (M_w/M_n < 2.5). There is no indication of any negative influence of the borane group on the metallocene polymerization.

The borane groups incorporated in polyolefins were interconverted to various functional (polar) groups. One common reaction is to convert borane groups to the corresponding hydroxy (OH) groups by reacting with $NaOH/H_2O_2$ reagents at 40 °C for 1 h. Despite the heterogeneous reaction condition in forming the corresponding hydroxylated PE−OH and PP−OH polymers, the interconversion reaction was highly effective due to the high surface area of borane groups in the semicrystalline microstructure of the PE and PP copolymers. The borane groups in the flexible side chains shall be located in amorphous phases where the chemical reagents can be easily reached. As will be discussed later, these

dx.doi.org/10.1021/ma401244t | *Macromolecules* 2013, 46, 6671−6698

Scheme 5. Functionalization of Polyolefin Using the "Reactive" *p*-MS Comonomer

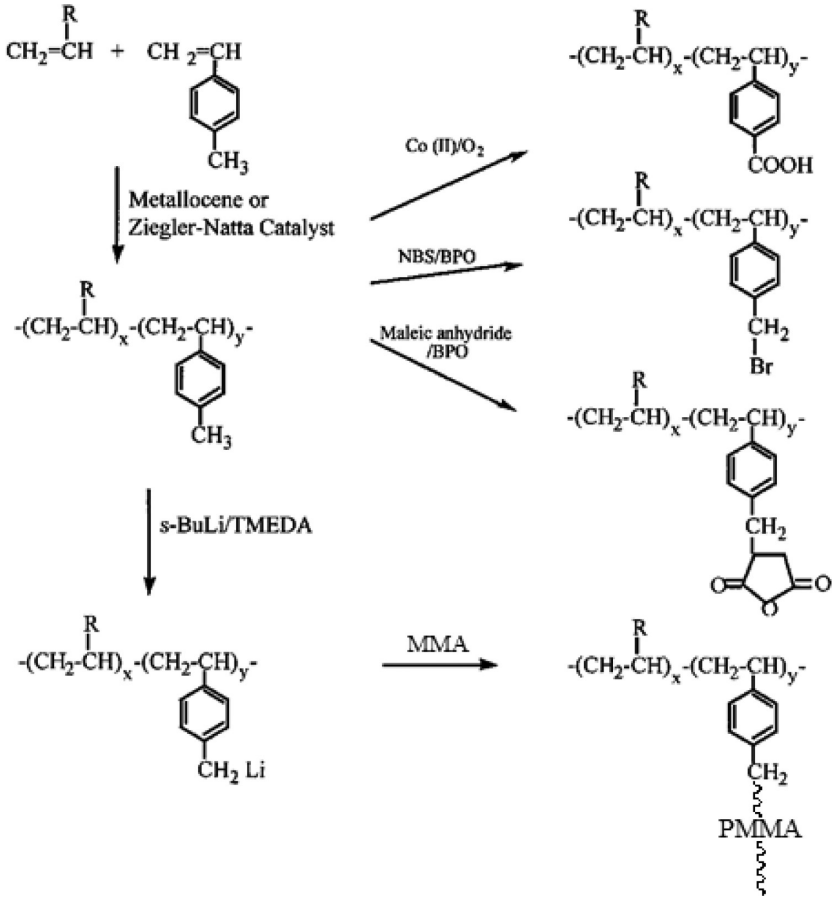

Scheme 6. Steric Jamming during the Crossover Reaction from *p*-MS to Propylene Incorporation (Reproduced with Permission from Ref 86. Copyright 1999 Wiley-VCH)

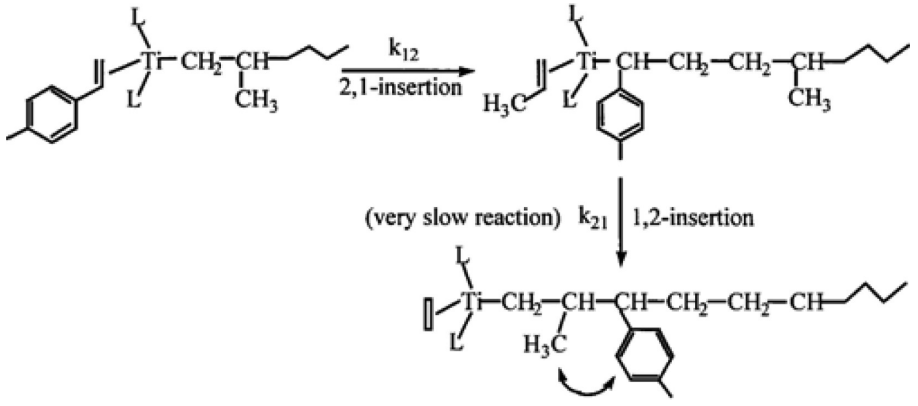

flexible functional (polar) groups in PE and PP exhibit unique properties in capacitor and polyelectrolyte applications.

On the basis of the same three considerations (i.e., stability, solubility, and versatility) of the "reactive" comonomer, we also investigated *p*-methylstyrene (*p*-MS) that contains "reactive" benzylic protons (φ-CH_3).[84−89] The major advantages of *p*-MS are its commercial availability, easy incorporation into the polyolefin, and versatility in the functionalization chemistry[90,91] under various reaction mechanisms, including free radical, cationic, and anionic processes. The benzylic protons are known to be facile in many chemical reactions, such as halogenation,[92−94] metalation,[95] and oxidation,[96] to form desirable functional group at the benzylic (φ-CH_3) position under mild reaction conditions, as illustrated in Scheme 5. It is interesting to note the negligible reactivity at the benzylic (methine) proton in the polymer chain for all reactions, suggesting a conformational control of the polymer chain on the chemical reactivity of the methine proton.

The ethylene/*p*-MS copolymerization reactions[84,85] were carried out using various metallocene catalysts, including $[(\eta^5\text{-}C_5Me_4)SiMe_2\text{-}(\eta^1\text{-}NCMe_3)]TiCl_2$, $Et(Ind)_2ZrCl_2$, and Cp_2ZrCl_2. As expected, the copolymerization efficiency follows the sequence of $[(\eta^5\text{-}C_5Me_4)SiMe_2\text{-}(\eta^1\text{-}NCMe_3)]TiCl_2$ > $Et(Ind)_2ZrCl_2$ > Cp_2ZrCl_2. The spatial opening at the active

dx.doi.org/10.1021/ma401244t | *Macromolecules* 2013, 46, 6671−6698

Scheme 7. New Reaction Mechanism To Prepare PP

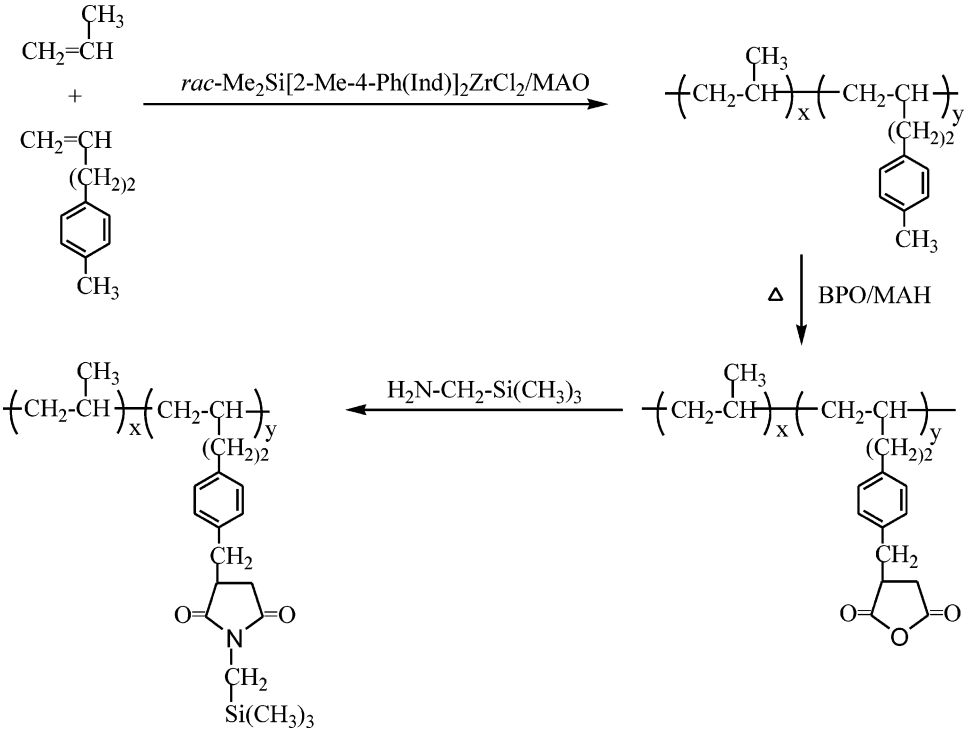

site of $[(\eta^5\text{-}C_5Me_4)SiMe_2\text{-}(\eta^1\text{-}NCMe_3)]TiCl_2$/MAO offers a high *p*-MS conversion and copolymers with a broad range of *p*-MS concentrations. In general, the catalyst activity systematically increases with the increase of *p*-MS content due to the improvement of the monomer diffusion in the lower crystalline copolymer structures. The resulting poly(ethylene-*co*-*p*-methylstyrene) (PE-*co*-*p*-MS) copolymers show narrow molecular weight (M_w/M_n = 2−3) and composition distributions. The melting point (T_m) and crystallinity (χ_c) of the copolymer are strongly relative to the density of the *p*-MS comonomer; the higher the density, the lower the T_m and χ_c. Only a single crystalline peak in the DSC curve was observed throughout the entire composition range, and the melting peak completely disappears at ∼10 mol % of *p*-MS concentration. The systematic decrease of the T_m and χ_c values in the PE copolymers implies a homogeneous reduction of PE consecutive sequences, which is consistent with a single-site copolymerization mechanism.

The copolymerization of propylene and *p*-MS[86] was investigated using isospecific metallocene catalysts, including *rac*-$Me_2Si[2\text{-}Me\text{-}4\text{-}Ph(Ind)]_2ZrCl_2$ and *rac*-$Et(Ind)_2ZrCl_2$. It was very unexpected to observe both catalysts as ineffective in the propylene/*p*-MS copolymerization, completely opposite to the corresponding ethylene/*p*-MS reaction. The presence of even a small amount of *p*-MS in PP cases shows severely reduced catalyst activity. As illustrated in Scheme 6, the drastic difference is attributed to the steric jamming phenomenon[71] in the crossover reaction from *p*-MS to propylene.

It is well-known that in metallocene catalytic polymerization the insertion of the styrene monomer is predominately a 2,1-insertion,[97−99] while the 1,2-insertion of the propylene monomer is dominant. Once the propagating PP chain has a chance to react with the *p*-MS monomer via a 2,1-insertion, the bulky *p*-phenyl group in the last unit of the growing chain is adjacent to the central metal atom and blocks the upcoming 1,2-insertion of a propylene unit. Since the homopolymerization of *p*-MS via the metallocene coordination mechanism is known to be near zero,[85] the metallocene active site at the *p*-MS unit dramatically slows the propagation process. This steric jamming problem was overcome by introducing a small spacer in the *p*-MS comonomer, as shown in Scheme 7. The new *p*-(3-butenyl)toluene (*p*-BT) comonomer contains a α-olefin moiety (instead of styrene) and "reactive" benzylic protons (φ-CH_3). The similar α-olefin moieties in both propylene and *p*-BT monomers offer a favorable metallocene-mediated copolymerization to form PP-*co*-*p*-BT copolymers with a broad range of *p*-BT content and narrow molecular weight and composition distributions.

The *rac*-$Me_2Si[2\text{-}Me\text{-}4\text{-}Ph(Ind)]_2ZrCl_2$/MAO mediated propylene/*p*-BT copolymerization results[100] are very different from those using the *p*-methylstyrene (*p*-MS) comonomer feed, showing almost no catalyst activity. Evidently, the α-olefin moiety in the *p*-BT comonomer (vs styrenic moiety in *p*-MS) provides effective comonomer incorporation in the *rac*-$Me_2Si[2\text{-}Me\text{-}4\text{-}Ph(Ind)]_2ZrCl_2$ mediated propylene copolymerization. The reactivity ratios of propylene (r_1) and *p*-BT comonomer (r_2) in this metallocene-mediated copolymerization are r_1 = 1.535 and r_2 = 0.425, with $r_1 \times r_2$ = 0.65, indicating a relatively good random copolymerization reaction with a slightly higher propylene reactivity. Even a small amount of comonomer incorporation (1 mol %) has a significant effect on the melting temperature (T_m) and heat of fusion (ΔH) of polypropylene, indicating the homogeneous distribution of bulky comonomers in the resulting copolymers. In addition, all PP-*co*-*p*-BT copolymers show high molecular weight and narrow molecular weight distribution (discussed later). The similar propylene/*p*-BT copolymerization mediated by heterogeneous Ziegler−Natta catalyst only results in the copolymer with low *p*-BT comonomer content and broad composition and molecular weight distributions. The reactivity ratios of

dx.doi.org/10.1021/ma401244t | *Macromolecules* 2013, 46, 6671−6698

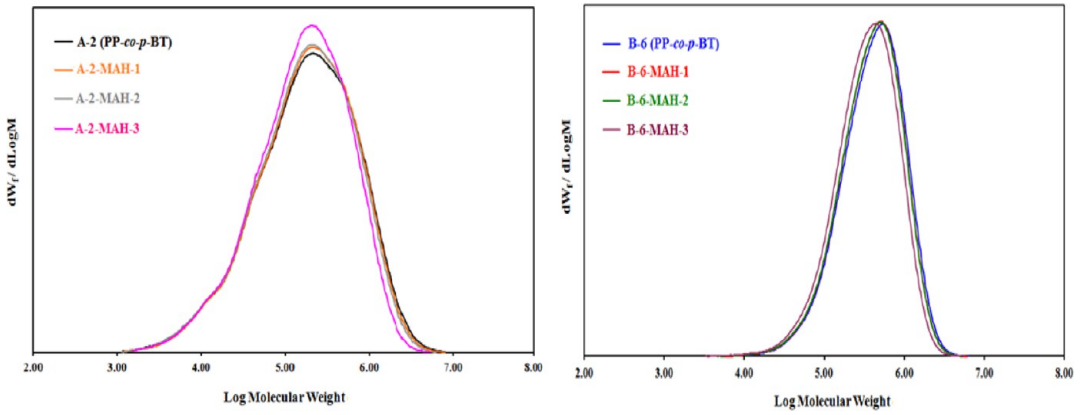

Figure 2. Absolute GPC (LS) curves (left) for starting PP-*co*-p-BT and three corresponding PP-*co*-MAH copolymers with 0.29, 0.76, and 0.90 wt % MAH contents (set A) and (right) starting PP-*co*-p-BT and three corresponding PP-*co*-MAH copolymers with 0.37, 1.0, and 1.1 wt % MAH contents (set B). Reproduced with permission from ref 100.

Scheme 8. Metallocene-Mediated Copolymerization of Propylene and *p*-(3-Butenylstyrene) and the Subsequent Thermal Functionalization and Cross-Linking Reactions

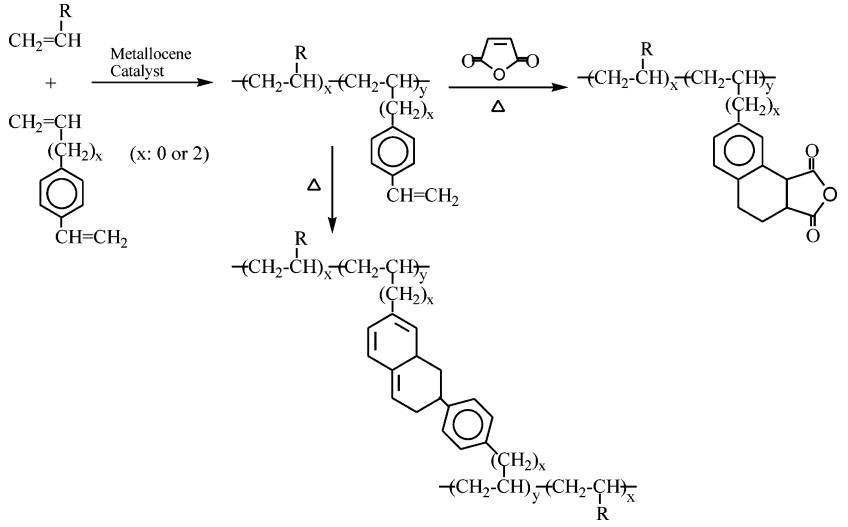

propylene (r_1 = 23.638) and the *p*-BT comonomer (r_2 = 0.75) in $TiCl_3$·AA/Et_2AlCl mediated copolymerization indicate the strong tendency of propylene consecutive insertion.

The primary goal of incorporating φ-CH_3 moieties in the polyolefin (either *p*-MS or *p*-BT comonomers) is versatility in accessing a broad range of functional groups, as illustrated in Schemes 5 and 7. The benzylic protons are ready for many chemical reactions, such as halogenation, oxidation, and metalation. Many functionalization reactions take place exclusively at the φ-CH_3 moieties, and the extent of functionalization is governed by the concentration of comonomers. One example (Scheme 7) is the free radical mediated maleic anhydride (MAH) grafting reaction to prepare maleic anhydride modified polypropylene (PP-*co*-MAH), which is the most important material for improving PP interactive properties in blends and composites. However, as illustrated in Scheme 2, current commercial PP-MAH polymers exhibit many structural defects, including low molecular weight (<20 kg/mol), deep color (impurities), MAH oligomers, and other defects due to chemistry difficulties. It is very important to develop a new method that can prepare a high PP-*co*-MAH polymer with a well-controlled molecular structure.

Figure 2 compares absolute GPC (LS) curves, using a light scattering (LS) detector to determine the absolute polymer molecular weight,[100] of two reaction sets involving two starting PP-*co*-*p*-BT copolymers, prepared by heterogeneous Ziegler–Natta catalyst and homogeneous metallocene catalyst, respectively, and their corresponding functionalized PP-*g*-MAH polymers. Figure 2 (left) compares GPC curves of set A samples, including the starting PP-*co*-*p*-BT copolymer (with 1 mol % *p*-BT units) prepared by the heterogeneous Ziegler–Natta and three corresponding PP-*g*-MAH polymers (with 0.29, 0.76, and 0.90 wt % MAH contents). Figure 2 (right) compares GPC curves of set B samples, including the starting PP-*co*-*p*-BT copolymer (with 1.3 mol % *p*-BT units) prepared by the homogeneous metallocene catalyst and three corresponding PP-*co*-MAH polymers (with 0.37, 1.0, and 1.1 wt % MAH contents). Before GPC measurements, the MAH groups in all PP-*co*-MAH polymers were converted to MAH–CH_2–$Si(CH_3)_3$ groups to prevent polymer chain interactions. All polymers in set B show very high molecular weights with narrow molecular weight distributions (PDI ~2.1); the molecular weight difference before and after the MAH modification is extremely minimal. Similarly well-controlled MAH grafting reactions were also observed in set A, with the

dx.doi.org/10.1021/ma401244t | *Macromolecules* 2013, 46, 6671–6698

exception of a broad molecular weight distribution (PDI > 4.8) with a low molecular weight shoulder shown in all polymers, which are indicative of the starting PP-*co*-*p*-BT copolymer being prepared by the heterogeneous Ziegler–Natta catalyst. It is important to note that these polymers also exhibit a broad composition distribution. Most of the reactive *p*-BT groups and the subsequent incorporated MAH moieties are located in low molecular weight polymers that have highly undesirable molecular structures serving as the interfacial agents.

Overall, we have addressed a long-standing scientific challenge and industrially important issue in the free radical maleic anhydride grafting reaction of polypropylene to prepare a desirable PP-*co*-MAH molecular structure with high molecular weight, narrow molecular weight, and composition distributions, a single MA grafting unit, and a controlled amount of MAH content. The newly designed PP-*co*-*p*-BT "reactive" copolymer can be effectively prepared by metallocene-mediated propylene copolymerization to form a broad composition range, high molecular weight, and narrow molecular weight and composition distributions. The reactive φ-CH_3 moieties offer selective MAH grafting reaction with the single MAH unit. The resulting PP-*co*-MAH polymers essentially keep their similar molecular weight as the starting PP-*co*-*p*-BT copolymer, and the content of the single enchained MAH unit is controlled by the *p*-BT comonomer concentration, the free radical initiator, and reaction time. These new PP-*co*-MAH polymers shall effectively increase PP interactive properties in many applications.

In addition, we had also studied asymmetric diene comonomers that contain a α-olefin and a styrenic moiety,[101−103] as illustrated in Scheme 8. The objective is to incorporate pendant styrene groups into the polyolefin flexible side chains, which are facile for a broad range of reactions, including free radical, cationic, and anionic functionalization and grafting reactions. With the versatility of metallocene catalysis, it is possible to select an active site with a specific stereo-opening that exhibits selectivity in the α-olefin enchainment and results in pendent styrene groups, without causing branching and/or cross-linking side reactions. As shown in Scheme 8, the pendent styrene groups in the polyolefin copolymer can engage in simple thermal cycloaddition with maleic anhydride to form the MAH-functionalized polyolefin or between styrene groups (dimerization) to form cross-linked polyolefin under a control manner.

The *rac*-CH_2(3-*t*-Butyl-Ind)$_2ZrCl_2$/MAO catalyst was found to be a selective metallocene catalyst for α-olefin enchainment, without reacting with styrene moiety.[103] All copolymerization reactions between propylene and *p*-(3-butenylstyrene) (*p*-BSt) maintained very high catalyst activities, and the resulting PP-*co*-*p*-BSt copolymers (with up to 8 mol % of *p*-BSt content) were completely soluble in xylene at an elevated temperature. However, the solution-cased PP-*co*-*p*-BSt copolymer films were cross-linked upon heating, due to a Diels–Alder [2 + 4] cycloaddition reaction between two pending styrene units (Scheme 8).[104] The resulting cross-linked PP (x-PP) films were subjected to a vigorous solvent extraction to remove the soluble fraction that was not fully cross-linked into the network structure. Figure 3 compares the gel content after thermal treatment for 1 h under various temperatures for three PP–BSt copolymers with various pendent styrene contents.[104] The cross-linking reaction starts at a relatively low temperature (~80 °C), and the rate is highly dependent on the temperature and *p*-BSt content. In the low temperature range <160 °C (below melting temperature), the cross-linking efficiency of the

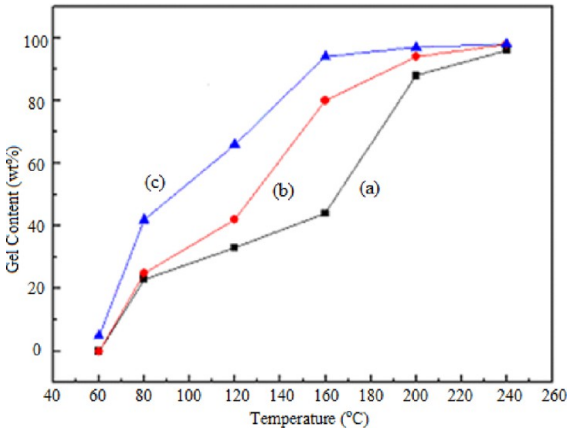

Figure 3. Gel content after thermal treatment for 1 h under various temperatures for three PP-*co*-p-BSt copolymers with pendent styrene concentration of (a) 0.42, (b) 0.73, and (c) 8.6 mol %, respectively. Reproduced with permission from ref103.

PP-*co*-*p*-BSt copolymer is dependent on the concentration of pendent styrene units. High cross-linker content is needed in order to observe an appreciable cross-linking reaction. It appears that it is important to anneal the copolymer film >160 °C (beyond its melting temperature) to achieve a high cross-linking efficiency, which is particularly important for the PP-*co*-*p*-BSt copolymer with <1 mol % of pendent styrene units. Beyond 200 °C, the interchain reaction can effectively take place. Despite only 0.42 mol % cross-linkers, the PP-*co*-*p*-BSt copolymer exhibits a near-complete cross-linked x-PP product.

3.4. "Reactive" Chain Transfer Agent Approach. As illustrated in Scheme 9, the "reactive" comonomer approach

Scheme 9. General Reaction Route To Prepare the Chain End Functionalized Polyolefins and Diblock Copolymers Using the Reactive Chain Transfer Approach

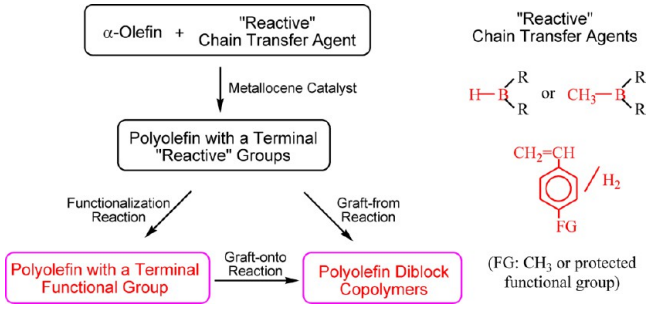

was expanded to a "reactive" chain transfer approach to prepare polyolefin containing a terminal functional group and polyolefin diblock copolymers.[71] With the advantage of a well-defined polymerization mechanism, our thought was to introduce a suitable "reactive" chain transfer agent that can be selectively incorporated at the polyolefin chain end during the polymer chain-releasing step from the active site. The *in situ* formed "reactive" terminal group can be effectively interconverted to a terminal functional (polar) group or used as an initiator to form a functional polymer chain under a mild reaction condition. The resulting chain end functionalized polyolefin and polyolefin diblock copolymer will not only provide hydrophilic (polar) properties but also preserve the intrinsic polyolefin properties, such as hydrophobicity, glass transition temperature, and melting temperature. The possi-

dx.doi.org/10.1021/ma401244t | *Macromolecules* 2013, 46, 6671−6698

bility is even more intriguing considering the difficulty in preparing the chain end functionalized polyolefin[105] and polyolefin diblock copolymers[106] as well as their potential applications.

In the past few years, we have discovered two classes of "reactive" chain transfer agents. The first family includes various organoborane compounds containing H−B and CH_3−B moieties[107−111] that can engage in a facile chain transfer reaction during many metallocene-mediated α-olefin polymerization reactions. The second one involves a styrenic moiety, which requires some selected metallocene catalysts in the presence of H_2.[112−114]

Scheme 10 illustrates the reaction mechanism involving organoborane chain transfer agents. Given the facile ligand exchange between B−H (or B−CH_3) bonds and most metal−alkyl groups, it would be logical to expect a fast chain transfer reaction to take place in most metallocene catalyst systems. In the presence of a borane chain transfer agent containing a B−H (or B−CH_3) group, the metallocene-mediated propagating polyolefin chain engages in a facile ligand exchange reaction between C−M (M = transition metal) and B−H or (B−CH_3) bonds due to the favorable acid−base interaction between the cationic metal center and anionic hydride. This ligand exchange reaction results in a borane-terminated polyolefin and a new active site that can reinitiate polymerization. The resulting borane-terminated polyolefin can be converted into a hydroxy-terminated polyolefin by treating it with $NaOH/H_2O_2$. There are some significant differences in applying the borane chain transfer agent containing B−H and B−CH_3 groups. Although the B−H group is more reactive toward the propagating polymer chain with a higher chain transfer constant, there are two potential side reactions that can derail the catalytic cycle, namely hydroboration of the olefin monomer and ligand exchange reactions between the borane and aluminum cocatalyst. Fortunately, borane compounds containing B−H groups usually form stable dimers that are unreactive toward olefins in typical olefin polymerization solvents (e.g., hexane, toluene). To eliminate the concern of a ligand exchange reaction between B−H and Al−alkyl, we have found two solutions—either applying perfluoroborate cocatalyst or using pure MAO with a low reaction temperature (<35 °C).

Scheme 10. Synthesis of a Chain Functional Polyolefin Using a Borane Chain Transfer Agent

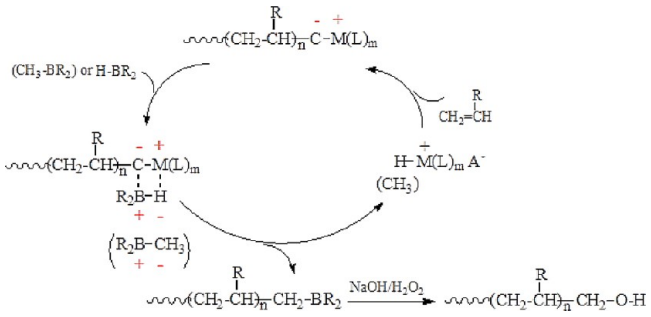

Figure 4 compares the plot of borane-terminated PE (PE-t-B) molecular weight (M_n) against the mole ratios of [ethylene]/[borane], which involve two borane CT agents, including 9-borabicylcononane (9-BBN) and dimesitylborane ($HB(Mes)_2$), and three metallocene catalysts, including $[C_5Me_4(SiMe_2N^tBu)TiMe]^+[MeB(C_6F_5)_3]^-$, $[(Ind)_2ZrMe]^+[MeB(C_6F_5)_3]^-$, and $[Cp^*_2ZrMe]^+[MeB(C_6F_5)_3]^-$.[109] In Figure 4 (left), the polymer molecular weight is almost linearly proportional to both molar ratios of [ethylene]/[9-BBN] and [ethylene]/[H-B$(Mes)_2$]. It is clear that the chain transfer reaction to the dialkylborane molecule (with rate constant k_{tr}) is the dominant termination process and that it competes with the propagating reaction (with rate constant k_p). The degree of polymerization (X_n) follows the simple comparative equation $X_n = k_p[\text{olefin}]/k_{tr}[\text{dialkylborane}]$ with the chain transfer constant $k_{tr}/k_p \sim 1/75$ and 1/137 for 9-BBN and H−B$(Mes)_2$, respectively. The cationic nature of the catalyst site, in combination with the stronger Lewis acidity of 9-BBN, is reflected in its higher reactivity with 9-BBN than H-B$(Mes)_2$ during the chain transfer reactions, as illustrated in Scheme 10.

It is interesting to understand the effects of the catalyst to the B−H chain transfer reaction, particularly regarding the steric and electronic roles at the active site on the rate of chain

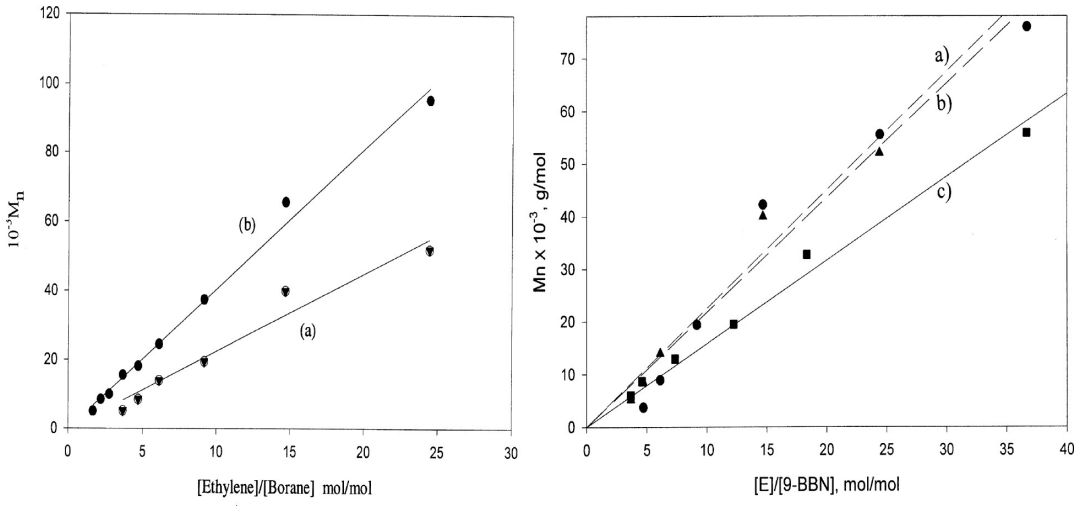

Figure 4. Plots of number-average molecular weight (M_n) of PE-t-B polymers versus the [ethylene]/[borane] mole ratios, with the comparison (left) between two borane CT agents (a) 9-BBN and (b) H-B$(Mes)_2$ and (right) among three metallocene catalysts (a) $[Cp^*_2ZrMe]^+[MeB(C_6F_5)_3]^-$, (b) $[(Ind)_2ZrMe]^+[MeB(C_6F_5)_3]^-$, and (c) $[C_5Me_4(SiMe_2N^tBu)TiMe]^+[MeB(C_6F_5)_3]^-$. Reproduced with permission from ref 109.

dx.doi.org/10.1021/ma401244t | Macromolecules 2013, 46, 6671−6698

Scheme 11. Synthesis of PP-t-p-MS Polymer Using a Styrenic Chain Transfer Agent (Reproduced with Permission from Ref 112)

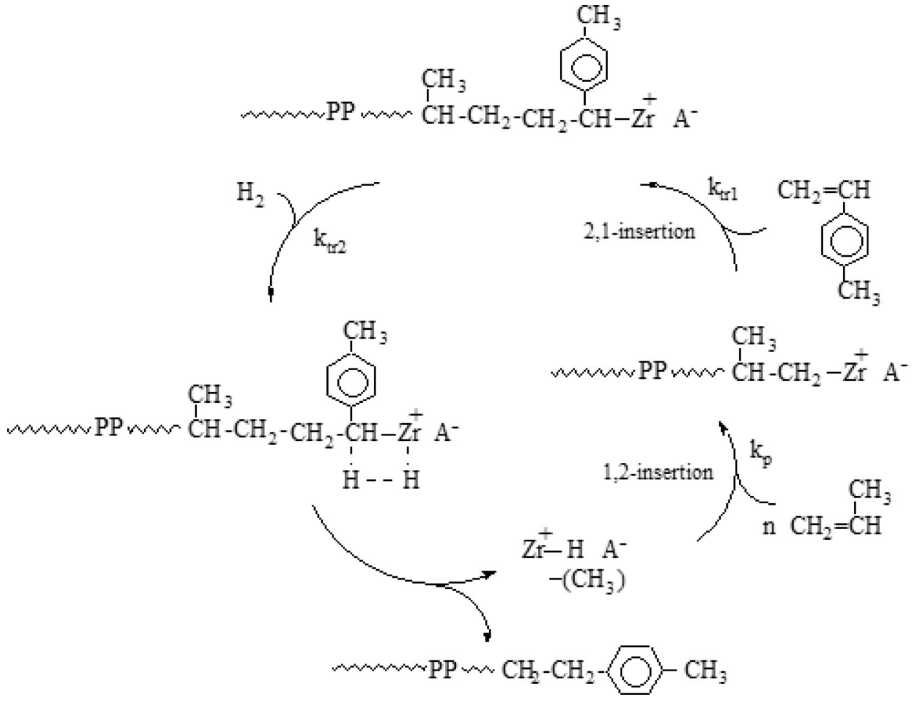

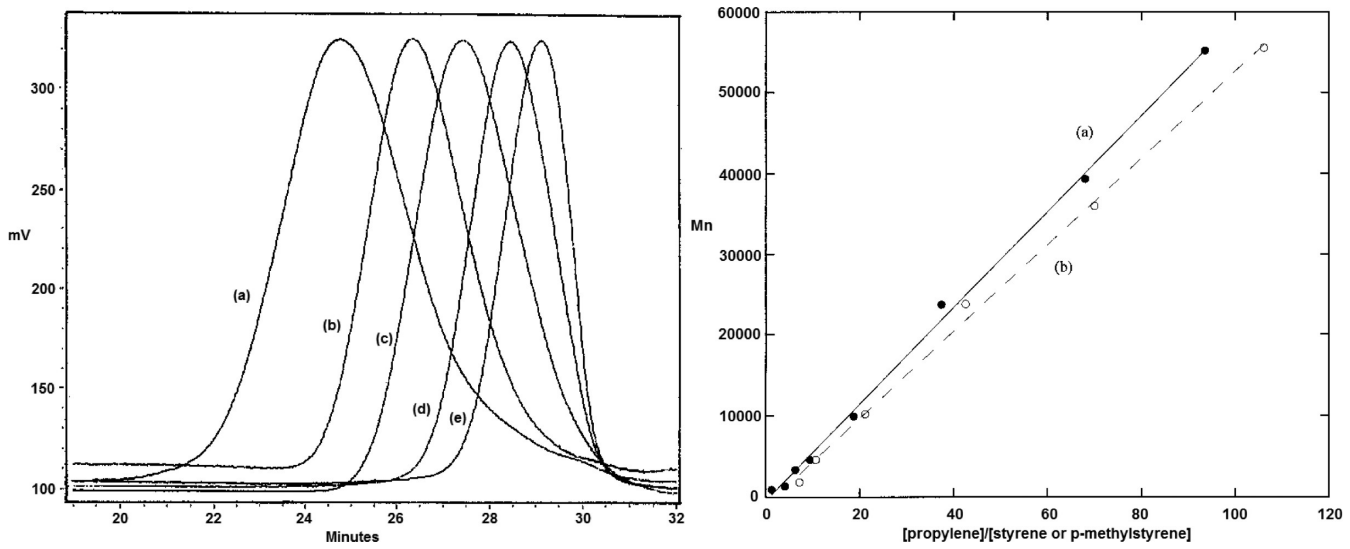

Figure 5. (left) GPC curves of (a) PP and several PP-t-*p*-MS polymers and (right) the plots of number-average molecular weights (M_n) of (a) PP-t-St and (b) PP-t-*p*-MS polymers versus [propylene]/[styrene] and [propylene]/[*p*-MS], respectively. Reproduced with permission from ref 112.

transfer reaction. Figure 4 (right) compares three linear plots of polymer molecular weight versus the [ethylene]/[9-BBN] mole ratio, using two sandwiched metallocene catalysts, including $[Cp^*_2ZrMe]^+[MeB(C_6F_5)_3]^-$ and $[(Ind)_2ZrMe]^+[MeB(C_6F_5)_3]^-$, and a constrained geometry $[C_5Me_4(SiMe_2N^tBu)TiMe]^+[MeB(C_6F_5)_3]^-$ catalyst. The first two active sites with small spatial openings show relatively low chain transfer activities with $k_{tr}/k_p \sim 1/75$. On the other hand, the last one with an opened active site exhibits significantly higher chain transfer activity with $k_{tr}/k_p \sim 1/57$. The spatial opening at the active site does affect the chain transfer reaction; however, the electronic contribution is unclear.

Overall, this method provides an effective and convenient route to prepare chain end functionalized polyolefins with controlled polymer molecular weights, which are very difficult to prepare by other methods. With the proper choice of borane chain transfer agents, metallocene catalyst systems, and reaction conditions, the chemistry can be applied to a broad range of polyolefin homo- and copolymers, such as polyethylene, polypropylene, syndiotactic polystyrene, poly(ethylene-*co*-propylene), poly(ethylene-*co*-1-octene), and poly(ethylene-*co*-styrene).[107−111] The molecular weight of the borane-terminated polyolefin is essentially inversely proportional to the molar ratio of [borane]/[olefin]. In turn, the terminal borane group is very reactive, which can be quantitatively converted to various functional groups and also can be selectively oxidized to form a stable polymeric radical for the living free radical polymerization of functional monomers (discussed later).

dx.doi.org/10.1021/ma401244t | *Macromolecules* 2013, 46, 6671−6698

Furthermore, intriguing is the expansion of the chain transfer methodology to styrenic molecules that usually serve as monomers during polymerizations. The research stems from an observation of steric jamming[86] (Scheme 6) during the copolymerization of propylene and *p*-MS using the *rac*-$SiMe_2$[2-Me-4-Ph(Ind)]$_2ZrCl_2$/MAO complex. As shown in Scheme 11, we took advantage of the dormant propagating site to prepare PP polymer with a terminal *p*-MS group. Although the catalytic Zr−C site in the propagating site becomes inactive to both propylene and *p*-MS, the dormant Zr−C site can react with hydrogen to form *p*-MS terminated polypropylene (PP-t-*p*-MS) and regenerate a Zr−H species that is capable of reinitiating the polymerization of propylene and continuing the polymerization cycles.[112]

Figure 5 (left) shows the typical GPC curves of a systematic set of PP-t-*p*-MS polymers prepared by the *rac*-Me_2Si[2-Me-4-Ph(Ind)]$_2ZrCl_2$ mediated propylene polymerization with various amounts of the *p*-MS/hydrogen chain transfer agent. The polymer's molecular weight distribution maintains narrow (M_w/M_n = ∼2), and the average molecular weight decreases with an increase in *p*-MS concentration. Figure 5 (right) compares the plot of the polymer molecular weight (M_n) versus the mole ratios of [propylene]/[p-MS] and [propylene]/[St]. Both show a linear proportionality between the polymer molecular weight and molar ratio of [propylene]/[*p*-MS] or [propylene]/[St], with very high chain transfer constant k_{tr}/k_p ∼ 1/6.4 and 1/7.5 for *p*-MS and styrene, respectively.[112] It is clear that the chain transfer reaction to the styrenic molecule is the dominant termination process. The cationic nature of the catalyst site is reflected in its higher reactivity to *p*-MS than styrene during the chain transfer reactions. The PP-t-*p*-MS polymer with just a few thousand molecular weight can be obtained. The catalyst activity was also proportionally depressed with the concentration of *p*-MS (or styrene), which reflects the competitive coordination at metallocene active sites between monomer and chain transfer agents.

The same *rac*-Me_2Si[2-Me-4-Ph(Ind)]$_2ZrCl_2$/MAO mediated chain transfer reaction scheme was applied to other styrene derivatives (St-f) that contain a functional (polar) group, such as Cl, OH, and NH_2. Three functionalized styrenic chain transfer agents were investigated, including *p*-chlorostyrene (St-Cl), dimethylisopropylsilane protected *p*-vinylphenol (St-OSi), and bis(trimethylsilane) protected *p*-ethylaminostyrene (St-NSi_2), as illustrated in Scheme 12. They result in the preparation of PP-t-St-Cl, PP-t-St-OH, and PP-t-St-NH_2 polymers with a terminal functional (polar) group.[114]

Scheme 12. Three Functional Styrenic Derivatives Used as the Chain Transfer Agents in the *rac*-Me_2Si[2-Me-4-Ph(Ind)]$_2ZrCl_2$/MAO Catalyzed Polymerization of Propylene

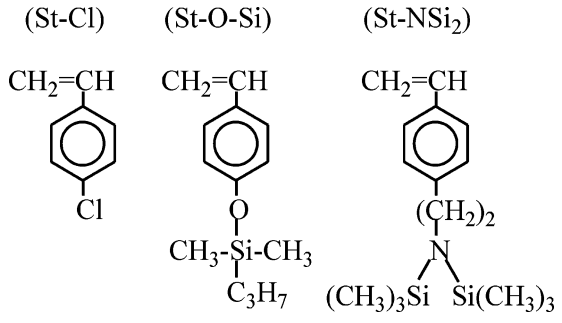

No external protection agent is needed for St-Cl. However, both the OH and NH_2 groups are highly sensitive to the *rac*-Me_2Si[2-Me-4-Ph(Ind)]$_2ZrCl_2$/MAO cationic site. The silane groups not only provide effective protection for both the OH and NH_2 functional groups during the metallocene catalysis but also can be completely deprotected by aqueous HCl solution during the sample work-up procedure. The overall reaction benefits especially from the very small quantity of the chain transfer agent needed in the preparation of high polymers. Therefore, the additional protection−deprotection step causes nearly no change in polymerization conditions. The plots of the polymer molecular weight (M_n) versus the molar ratio of [propylene]/[St-f], including all three St-Cl/H_2, St-OSi/H_2, and St-NSi_2/H_2 chain transfer agents, are all linearly proportional, with a chain transfer constant k_{tr}/k_p of 1/21 for St-Cl/H_2, 1/48 for St-OSi/H_2, and 1/34 for St-NSi_2/H_2, respectively.[114] It is worth noting that the k_{tr}/k_p values are significantly lower than those seen in styrene and *p*-MS cases under similar reaction conditions. The bulky, protected functional groups may reduce the frequency of the chain transfer reaction.

Overall, the experimental results strongly indicate a clean and effective reaction scheme. The combination of the facile *in situ* chain transfer to St-f/H_2 during the catalytic polymerization of propylene and the subsequent complete deprotection reaction during the sample work-up step affords an interesting reaction scheme in the preparation of the chain end functionalized i-PP with a Cl, OH, or NH_2 terminal group via a one-pot reaction process.

3.5. Synthesis of Polyolefin Block/Graft Copolymers.

In addition to the preparation of functional polyolefins with side chain and chain end functional groups, the reactive groups (i.e., borane, *p*-MS, and styrene moieties) in the polyolefin also provide convenient routes to prepare polyolefin graft and block copolymers, containing both a polyolefin block (PE, PP, *s*-PS, etc.) and functional polymer block (acrylic polymers), with good control of the molecular structure.[115−122] In other words, instead of obtaining a functional group from a reactive group, the same reactive group can produce a functional polymer chain with hundreds and thousands of polar groups, which significantly increases the efficiency of the reactive group. As illustrated in Scheme 13, the incorporated borane and *p*-MS groups have been transformed into living radical and anion macroinitiators, respectively, for initiating graft-from polymerization. On the other hand, the incorporated DVB unit resembles a styrene monomer that can involve the subsequent polymerization reactions.[123−125] A broad range of polyolefin graft and block copolymers have been prepared, which have high functional (polar) group concentrations without compromising desirable polyolefin properties, such as crystallinity, melting temperature, elasticity, etc. They have been shown to be highly effective interfacial agents to improve the compatibility of polyolefin blends and composites.

Scheme 13 (left) illustrates a borane-terminated PE (PE-t-B) (Scheme 10) that is transformed to the PE macroinitiator for forming a PE-b-PMMA diblock copolymer. The terminal borane group in PE can be spontaneously oxidized to a peroxide (B−O−O−C) moiety even at a very low temperature (−65 °C). Because of the unfavorable ring strain increase by inserting oxygen into the C−B bonds in the bicyclic ring of 9-BBN, which destroys the stable double chair-form structure, the oxidation reaction selectively takes place at the C−B bond in the linear alkyl group to produce peroxyborane (C−O−O−B).

dx.doi.org/10.1021/ma401244t | *Macromolecules* 2013, 46, 6671−6698

Scheme 13. (left) PE-*b*-PMMA Diblock Copolymer Prepared by PE-t-B Polymer (Macroinitiator) and a Borane-Mediated "Living" Radical Graft-from Polymerization and (right) PP-*b*-PS Diblock Copolymer Prepared by PP-t-*p*-MS Polymer (Macroinitiator) and a "Living" Anionic Graft-from Polymerization

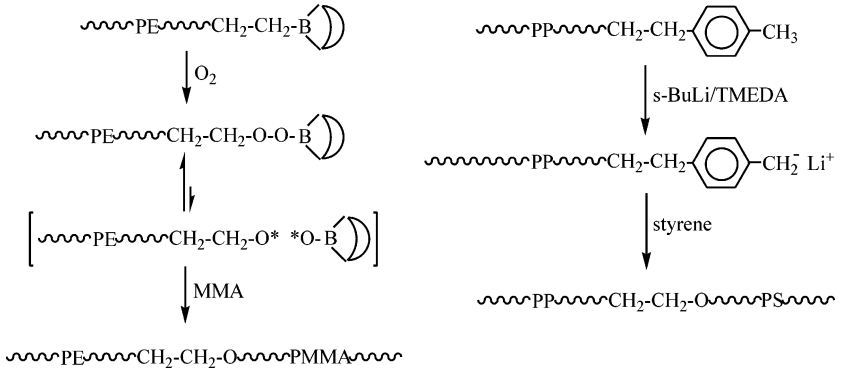

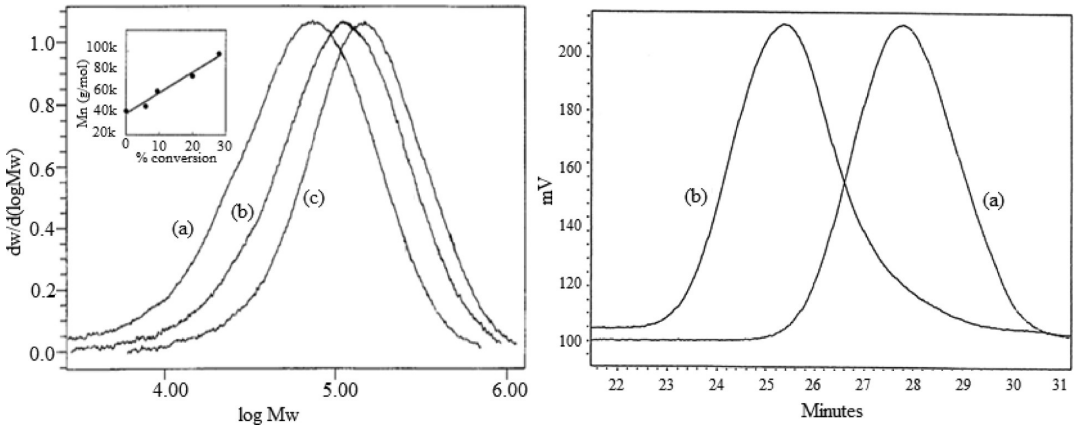

Figure 6. GPC curve comparison (left) between two PE-*b*-PMMA diblock copolymers with (a) M_n = 98 000 g/mol and M_w/M_n = 2.3 and (b) M_n = 62 000 g/mol and M_w/M_n = 2.4 and (c) the starting PE-t-B polymer (M_n = 43 000 g/mol and M_w/M_n = 2.2) and (right) (a) the starting PP-t-*p*-MS ($M_n = 26 \times 10^3$ g/mol and M_w/M_n = 2.3) and (b) the resulting PP-*b*-PS diblock copolymer ($M_n = 44 \times 10^3$ g/mol and M_w/M_n = 2.3). The inset shows the linear plot of polymer molecular weight versus the monomer conversion and compares the results with a theoretical line based on the polymer molecular weight estimated from [g of monomer consumed]/[mole of initiator]. A good match with the straight line through the origin strongly supports the "living" radical polymerization. Reproduced with permission from ref 112.

The peroxyborane behaves very differently from regular benzoyl peroxides and consequently decomposes by itself, even at ambient temperature. The decomposition reaction follows the homolytic cleavage of peroxide to generate an alkoxy radical (C−O*) and a borinate radical (B−O*). The alkoxyl radical (C−O*), located at the end of the polyolefin chain, is very reactive and can be used for the initiation of radical polymerization with the presence of free radical polymerizable monomers. On the other hand, the borinate radical (B−O*), stabilized by the empty p-orbital of boron through back-donating electron density, is too stable to initiate polymerization. However, the borinate radical may form a weak and reversible bond with the growing chain end during the polymerization reaction.[126,127] Upon the dissociation of the electron pairs in the resting state, the growing chain end can then react with monomers to extend the polymer chain to form the diblock copolymer. Overall, the reaction process resembles a transformation reaction from metallocene coordination polymerization to "living" free radical polymerization via a borane group at the polymer chain end. The reaction involves only one borane group per polymer chain. The entire reaction process provides the ultimate test for examining the efficiency of the borane reagent in the chain extension process.

On the other hand, the incorporated *p*-MS group in the polyolefin provides the active site to transform metallocene polymerization to living anionic polymerization.[112] Scheme 13 (right) illustrates the anionic reaction process from the PP-t-*p*-MS to the PP-*b*-PS diblock copolymer involving only one *p*-MS group per polymer chain. The metalation reaction of *p*-MS terminated polypropylene (PP-t-*p*-MS) was carried out under heterogeneous reaction conditions by suspending the powder form of PP in *sec*-BuLi/TMEDA/cyclohexane solution. To examine the efficiency of the reaction, some of the metalated polymer was terminated with $Cl-Si(CH_3)_3$ and examined by an ^1H NMR measurement, showing about 85% conversion. The lithiated PP-t-*p*-MS was used to prepare diblock copolymers. By mixing polymer powder with styrene monomer in cyclohexane solvent, the living anionic polymerization took place to produce PP-*b*-PS diblock copolymer. After the reaction, the product was vigorously extracted by refluxing THF to remove any PS homopolymer. In all cases (including high molecular weight PP-t-*p*-MS polymer cases), the soluble PS homopolymer fraction was negligible.

Figure 6 compares the GPC curves of two sets of diblock copolymers with their starting PE-t-B and PP-t-*p*-MS polymers. Despite the doubling of polymer molecular weight, the molecular weight distribution remains very constant and at

dx.doi.org/10.1021/ma401244t | *Macromolecules* 2013, 46, 6671−6698

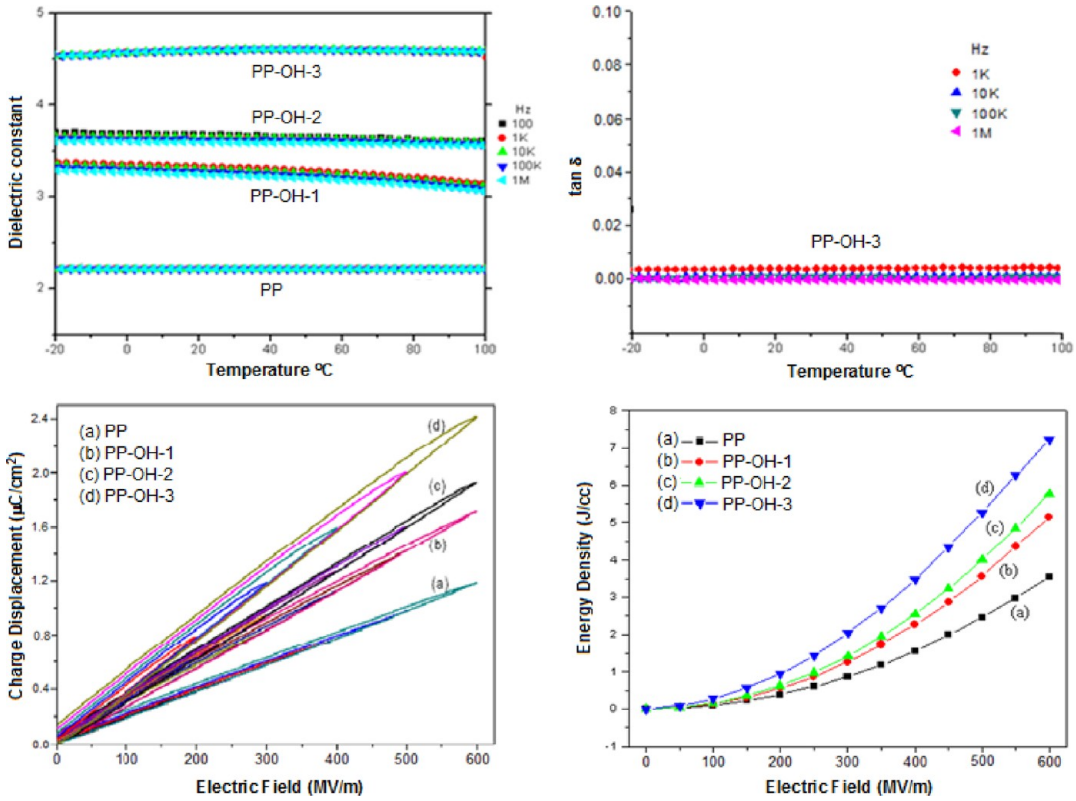

Figure 7. (top, left) Dielectric constants, (top, right) dielectric loss, (bottom, left) *D*–*E* loops, and (bottom, right) energy density for (a) PP and three PP-OH copolymers containing (b) 0.7, (c) 1.8, and (d) 4.2 mol % OH content. Reproduced with permission from ref 131.

narrow levels (M_w/M_n = 2.0–2.4). The monochromatic increase of the copolymer molecular weight, with only a slight broadening in the molecular weight distribution and no detectable PE or PP homopolymer, clearly points to the existence of a terminal reactive group at each polymer chain end and the living radical and anionic polymerizations in the chain extension process.

Summary and Future Perspectives: Polyolefin Functionalization. Overall, we have developed a powerful functionalization method with the combination of metallocene catalysis and reactive polyolefin approach. The technology involves several designed comonomers and chain transfer agents containing three reactive groups (i.e., organoborane, benzylic protons (φ-CH_3), and styrene moieties) that are stable with metallocene catalysts, have good solubility in the reaction media, and are versatile in the subsequent functionalization and graft-from reactions. In this functionalization process, metallocene catalysts provide the selective incorporation of reactive sites into the polyolefin side chains or chain end, and the incorporated reactive groups can be directly interconverted to various functional groups (OH, NH_2, etc.) or transformed into "living" radical or anionic macroinitiators to prepare block/graft copolymers. This transformation of active sites allows the preparation of each vinyl polymer segment with the most suitable chain-growth mechanism. In addition, the composition of polyolefin block/graft copolymers can be further expanded to polycondensation (step-growth) polymer chains by using the resulting functional polyolefins having OH and NH_2 groups for ring-opening polymerization or a coupling reaction with some polycondensation polymer chains with a suitable terminal group. In other words, it is possible to design and synthesize a broad range of well-defined functional polyolefin polymers with selective functional groups, concentrations, and locations. As will be discussed, the presence of hydrophilic functional polymer chains (or side chain groups) in the semicrystalline and highly hydrophobic polyolefin matrix results in a clear microphase-separated morphology with active interfaces and unique surface properties. They show multiple property functions and offer a new class of high performance and cost-effective materials. In the following sections, I will discuss how we took advantage of new polyolefin materials for several energy-related applications, with some advances in each area.

4. ENERGY APPLICATIONS

As discussed in section 1, polyolefins possess many desirable properties as well as shortcomings for specialty applications that usually require specific molecular structures and morphologies with multiple property functions. Considering the low cost and industrially established manufacturing and fabrication capabilities, it would be attractive to continue focusing on polyolefins and to apply newly available polyolefin chemistry to prepare desirable functional polyolefins with the designed molecular structures and morphologies to address such shortcomings. In the past decade, we have been taking advantage of new polyolefins for three energy-related research areas with some tangible results, which will be discussed and used as examples to illuminate the advantages of new functional polyolefin structures.

4.1. Functional Polyolefin-Based Capacitors. As discussed in section 2.2, biaxial-oriented polypropylene (BOPP) thin films are currently the state-of-the-art dielectrics in capacitors,[16−19] which can produce an energy density ~2 J/cm^3 after applying an external electric field (E = 500 MV/m). Despite the low energy density, BOPP capacitors offer reliable

dx.doi.org/10.1021/ma401244t | *Macromolecules* 2013, 46, 6671−6698

energy sources with low loss and cost-effectiveness. Currently, most capacitors are used as pulse power supplies and electric conditioners; they have insufficient energy density for many energy storage applications. Based on the energy density equation (eq 1), a defect-free PP film with a dielectric constant (ε = 2.2), thickness (d = 10 μm), and an applied voltage V = 5 kV (E = 500 MV/m) can offer a maximum energy density of 2 J/cm^3, similar to that of the experimental result. Theoretically, further increases in the dielectric constant (ε) and the applied electric field (E), while maintaining low dielectric loss, shall result in a higher energy density.

$$\text{energy density (J/cm}^3) = \frac{1}{2}\varepsilon\varepsilon_0 E^2 = \frac{1}{2}\varepsilon\varepsilon_0 (V/d^2)$$

(ε_0 is the permittivity of free space = 8.85×10^{-12} F/m) (1)

In the past decade, many research groups have been investigating various polymer dielectrics with the objective to increase dielectric constant (ε) and breakdown strength (E). However, the results are mixed at best.[128−130] So far, there is no suitable material that can achieve high energy density and low loss and no discussion about their processability, self-healing, long-term reliability, cost, etc. The ε value in the polymer is contributed by a combination of induced electronic polarization (σ and π electrons), ionization (ion pairs), and segmental motion (including dipole orientation). The low dielectric constant in BOPP is caused by a small σ electron polarization. It is clear that there is much room to improve BOPP dielectric properties. However, many attempts to increase the ε value come at the expense of great energy loss and generated heat that causes instability in the polymer film. Ideally, the dielectric loss shall keep very low (<1%) in polymer film capacitors. On the other hand, the breakdown strength (E) is strongly dependent on the polymer film quality (molecular weight, morphology, mechanical strength, uniformity of film thickness, impurities, defects, etc.). PP with a linear molecular structure exhibits low melt strength and presents a challenge in forming strong (defect-free) thin films (thickness <10 μm).

Our general research strategy has been to modify the PP polymer structure with selective incorporation of polarizable functionalities that can simultaneously improve its dielectric deficiencies while maintaining low loss and other desirable properties. In the past few years, we have been investigating two new PP polymers, including the hydroxylated polypropylene (PP-OH)[131] and cross-linked polypropylene (x-PP).[132] They were prepared by the reactive comonomer approach discussed in section 3.3 and exhibit an increase in the dielectric constant (ε) and breakdown strength (E) without showing negative effects to the desirable PP properties.

PP-OH Capacitors. Two types of PP-OH copolymers (Table 1), with taped and random copolymer microstructures, were prepared by heterogeneous Ziegler−Natta and homogeneous metallocene catalysts, respectively. The DSC curves clearly show the taped copolymers maintaining high T_m and crystallinity (χ), which were chosen for dielectric studies. Figure 7 shows the dielectric constant (ε), dielectric loss (tan δ), charge displacement−electric field (D−E) polarization loop, and energy density of three PP-OH taped copolymers (runs D-1, D-2, and D-3 in Table 1) containing 0.7, 1.8, and 4.2 mol % OH comonomer units, as well as the BOPP reference. The dielectric constant increases proportionally with the OH content. The ε value of PP-OH-3 with 4.2 mol % of the OH comonomer content reaches about 4.6 (more than 2 times that of BOPP) (Figure 7, top left). All PP-OH dielectric profiles resemble the PP profile, with a dielectric constant (ε) that is independent over a wide range of frequencies (between 100 and 1 M Hz) and temperatures (between −20 and 100 °C).[131] These overlapping and flat dielectric constant lines imply a fast polarization response for the PP-OH copolymer, even under a relatively low electric field condition. At the same time, we were pleasantly surprised to observe that all PP-OH copolymers also exhibit similar low dielectric loss. The PP-OH-4 with 4.2 mol % OH content (Figure 7, top right) shows dielectric loss tan δ < 0.003, over a wide temperature and frequency range. In close resemblance to BOPP, all PP-OH copolymers exhibit similar linear and slim D−E loops (Figure 7, bottom left); the slope of the D−E loop increases with the OH content, consistent with the dielectric results. The charge displacement of PP-OH-3 reaches 2.4 μC/cm^2 at 600 MV/m, which is double that of PP under the same applied electric field. Evidently, all results indicate reversible polarization, and the dielectric loss maintains very small with even the PP-OH copolymers exhibiting significantly higher dielectric activities.

Figure 7 (bottom, right) compares the energy density of the same four PP and PP-OH polymers. They are estimated from the D−E loops shown in Figure 7 (bottom, left). The total energy density (W_{charge}) charged to the capacitor is estimated by integrating the area $W_{charge} = \int E\, dD_{charge}$ in the charging cycle. The energy density ($W_{discharge}$) of the capacitor should be the total energy released during the discharging cycle, by integrating the area $W_{discharge} = \int E\, dD_{discharge}$. The difference, $W_l = W_{charge} - W_{discharge}$, is the energy loss ($W_l$), which is equal to the area enclosed by the charging and discharging cycle. The energy density clearly increases with the OH content and exponentially increases with the applied electric field (E). At the applied electric field E = 600 MV/m, the energy density for PP-OH-3 reaches 7.42 J/cm^3—more than triple that shown in BOPP capacitors.[131] Most importantly, the increase in energy density does not cause an increase in energy loss, which remains very low (similar to PP) for all PP-OH copolymers. The OH groups in the flexible side chains clearly contribute to the polarizability of the PP-OH at an unexpectedly large scale, which may originate from the induced electronic polarization of OH groups along with the local dipole orientation.

It is interesting to understand the positive effect of OH groups on a combination of dielectric properties. As illustrated in Figure 8, the flexible OH groups form interchain H-bondings with a network structure that provides reversible segment stability under the applied electric fields even when the temperature rises up to 100 °C.

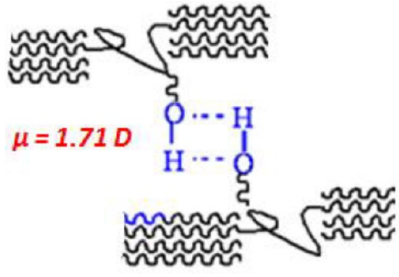

Figure 8. An illustration showing a network structure via H-bonding between OH groups.

dx.doi.org/10.1021/ma401244t | *Macromolecules* 2013, 46, 6671−6698

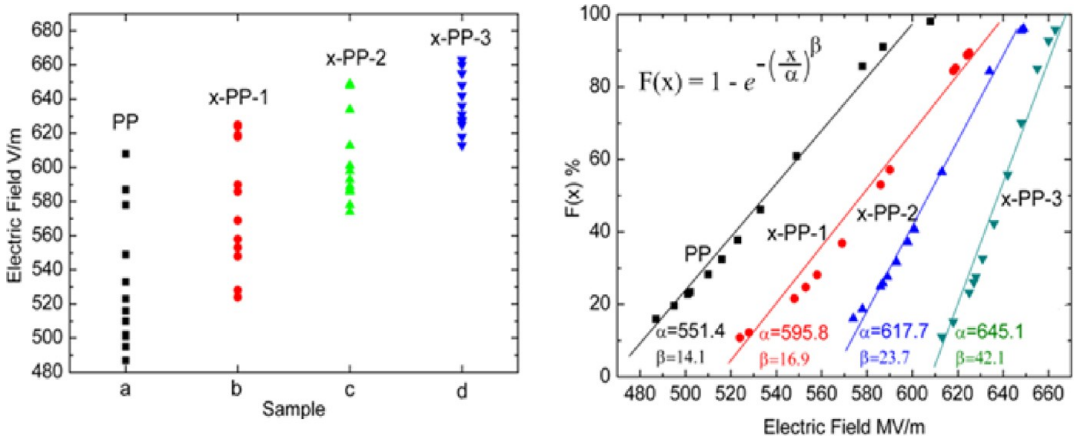

Figure 9. (left) Breakdown strength and (right) Weibull distribution for PP, x-PP-1, x-PP-2, and x-PP-3 dielectrics with 0.7, 1.4, and 2.1 mol % cross-linkers, respectively. Reproduced with permission from ref 132. Copyright 2011 American Institute of Physics.

x-PP Capacitors. The positive effects on the H-bonding (physical) network structure in the PP-OH dielectric prompt us to investigate the chemically cross-linked PP network structure (x-PP).[103] It is well-known that chemical cross-linking increases polymer mechanical strength and thermal stability, both which are highly important to dielectric breakdown strength (E) and long-term reliability. On the other hand, there was no chemical route that shows an effective cross-linking reaction between PP chains. For high electric field applications, the resulting x-PP shall contain no impurities that are detrimental to breakdown strength. As discussed in section 3.3, we have developed a unique method to prepare cross-linked polyolefins with high cross-linking efficiency and high purity (very important for dielectrics). Upon heating the PP-*co*-BSt thin film, the interchain cycloaddition takes place between two pendent styrene units to obtain x-PP dielectrics, without forming any byproduct.

Figure 9 (left) compares breakdown strength between three x-PP copolymers, containing 0.7, 1.4, and 2.1 mol % cross-linkers units, and the corresponding linear PP polymer. Figure 9 (right) shows their Weibull distributions with the estimated α and β values. All polymer films (thickness: 10−15 μm) were prepared by solution casting before thermal cross-linking. The chemical cross-linking feature has a significant effect to the breakdown strength and breakdown distribution—the higher the cross-linking density, the higher the breakdown strength (α value) and the narrower the distribution (β value).[132] The x-PP-3 thin film shows a breakdown strength between 620 and 670 MV/m with a α value = 645 MV/m, which is almost the same as that of biaxially oriented PP (BOPP) films that are carefully conditioned (through stretching and annealing) to increase chain orientation and crystallinity and to reduce defects. In addition, the x-PP-3 film exhibits a very narrow breakdown distribution with an exceptionally high β value of 42, indicating excellent dielectric reliability, which is an important quality in capacitors.

In addition, we also observed the systematic increase of the ε value in the x-PP dielectric with a level proportional to the BSt content. The value of ε = 3 for x-PP with 3.65 mol % of the BSt comonomer content is higher than the values (ε = 2.2) of BOPP. They also exhibit similar linear and slim $D-E$ loops; the slope of the $D-E$ loop increases with the BSt content. The BSt groups clearly contribute to the polarizability of the x-PP copolymer, which may be originated from the induced π-electronic polarization of aromatic groups that are added to the existing σ-electronic polarization (CH_3-CH groups) in the PP chain. The combination of a high dielectric constant (ε = 3), relatively high breakdown strength (645 MV/m), and low energy loss in the x-PP dielectric film offers a reliable energy density >5 J/cm^3, significantly higher than the 2 J/cm^3 typically shown in BOPP capacitors.

Challenges in Dielectric Energy Storage. Both PP-OH and x-PP polymers with only few percentages of OH and π-electron moieties show the tangible increase of the dielectric constant. The incorporated functional groups *in situ* forming a network structure provide the mechanism for reversible polarization-depolarization with slim $D-E$ loops and exhibit higher breakdown strength and narrower breakdown distribution. Compared to state-of-the-art BOPP capacitors, the new functional PP capacitors more than double the energy density (>5 J/cm^3) without showing an adverse effect on other desirable properties. However, considering the pulsed power needs in many military and civilian applications, with energy storage capacity >20 J/cm^3, there is a significant gap in realizing dielectric energy. The key challenge lies in the dielectric polymer that could simultaneously possess several key properties, including dielectric constant (ε >10), low dielectric loss (tan δ < 0.1%), high breakdown strength (E >800 MV/m), high operation temperature >150 °C, discharge time in millisecond (ms), and good reliability >8000 cycles. They shall also be cost-effective and easy to process into uniform thin films (<10 μm).

On the basis of the current experimental results, it should be theoretically possible to significantly increase energy density. If we had a polymer film with the combined properties of a dielectric constant ε = 20 (which has indeed been achieved in some functional moieties) with a breakdown strength E = 1000 MV/m (observed in some x-PP films), the result could be a theoretical energy density of 84 J/cm^3 at the material level. Some polarization mechanisms, either induced polarization from polar (or ionic) groups, π-electron delocalization, and/or dipole orientation, provide various avenues for increasing the dielectric constant. The combination of melt strength and film processing technology could prepare the strong and uniform thin film without defects or impurities, which could significantly increase breakdown strength (the theoretical breakdown strength for PP chain shall be far more than 1000 MV/m). Figure 10 shows a hypothetical $D-E$ loop with an antiferro-

dx.doi.org/10.1021/ma401244t | *Macromolecules* 2013, 46, 6671−6698

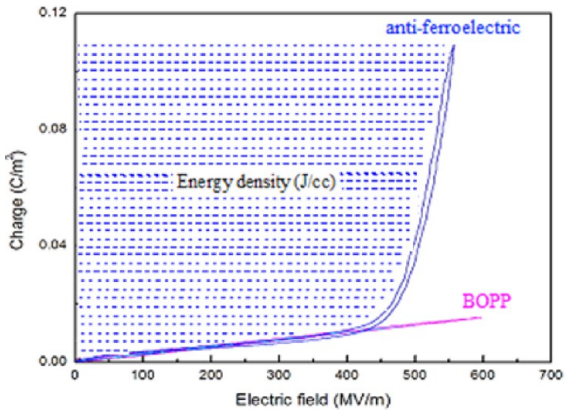

Figure 10. Comparison of $D-E$ loops between BOPP and an ideal (hypothetical) dielectric.

electric profile and late polarization at high fields as well as no remnant polarization at $E = 0$ and no coercive electric field at $D = 0$. Compared to the linear polarization shown in BOPP, PP-OH, and x-PP samples, this $D-E$ loop profile offers the maximum energy density (shaded area).

4.2. Functional Polyolefin-Based Ion Conductors. As discussed in section 2.3, microporous PE and PP films are commonly used as separators[20,21] in batteries, offering excellent electric insulation and good chemical and thermal stabilities. The semicrystalline and hydrophobic PE and PP matrixes are highly suitable material under demanding (chemically, electrochemically, and mechanically) electrochemical environments. However, it is very rare to see polyolefin-based ion conductors used as a solid polymer electrolyte (SPE)[133,134] or ion exchange membrane (IEM)[135−139] that can perform both separator and ion conductor functions. Several polymers, such as poly(ethylene oxide),[140−144] fluoropolymers,[145−147] polysulfones,[148−152] and cross-linked polystyrene,[153−155] are commonly used as the polymer backbones for preparing numerous SPE and IEMs. They show various advantages, however also some shortfalls. Poly(ethylene oxide) (PEO)-based SPE is restricted by the low ionic mobility and conductivity at ambient temperatures, partially due to crystallinity.[140−142] Fluoropolymers are generally expensive, and there are concerns in chemical stability[156,157] under strong base conditions. The preparation of polysulfones by the polycondensation process requires high chemical purity and a precise functional group stoichiometry in the monomers to achieve a desirable high molecular weight. The cross-linked polystyrene is usually prepared on reinforced backing fabrics to increase its mechanical strength. Because of the insolubility of ion exchange membranes, many ion incorporation procedures involve free radical grafting reaction[158−160] under a heterogeneous condition, which usually produces ill-defined molecular structures. Some functionalization routes to prepare anionic exchange membranes (AEMs) also involve carcinogenic chemicals.[161,162]

There have been several papers[163−167] that discuss the study of polyolefin-based IEMs. Most functionalization routes have been based on the postpolymerization process, involving irradiation-mediated free radical graft polymerization that results in highly complicated molecular structures, as discussed before. The polymer structure and morphology have rarely been characterized. Recently, a new synthesis route has emerged that uses metathesis polymerization process to prepare PE-based AEMs with well-controlled molecular structures. Coates et al.[168−170] employed a Grubbs second-generation Ru catalyst in the ring-opening metathesis polymerization (ROMP) of cyclooctene with various cyclooctenyl ammonium and phosphonium derivatives and the subsequent hydrogenation reaction to prepare solution-processable PE-based alkaline AEMs (without cross-linking). A desirable AEM with 1.5 mmol HO^-/g IEC value, insoluble in both pure water and aqueous methanol at 50 °C, exhibits mechanical strength of 6 MPa at break and high hydroxide and carbonate conductivities (65 and 30 mS/cm at 50 °C, respectively). Wagener et al.[171,172] also showed several regioregular PE-based ionomers containing imidazolium bromide groups, which are prepared by applying first- and second-generation Grubbs catalysts in acyclic diene metathesis polymerization (ADMET) with functional α,ω-diene monomers. The subsequent hydrogenation and quaternization reactions result in well-defined PE copolymers containing pendent ionic liquid moieties.

PE-$NR_3^+Cl^-$ and x-PE-$NR_3^+Cl^-$ Anion Exchange Membranes. Our research in studying AEMs stemmed from a hydrogen production program using a Cu−Cl thermochemical cycle.[173,174] For producing H_2 in the cathode of the CuCl−HCl electrolyzer, an efficient and selective Cl^- conductive AEM is essential for selective Cl^- ion diffusion from cathode to anode. As shown in Scheme 14, we have prepared PE-based AEMs

Scheme 14. Two Parallel Synthetic Routes To Prepare PE-$NR_3^+Cl^-$ and x-PE-$NR_3^+Cl^-$ Membranes

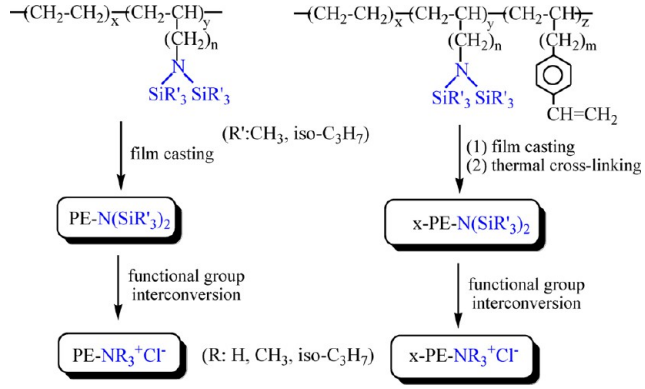

containing ammonium chloride ions (PE-$NR_3^+Cl^-$; R: H, CH_3, iso-C_3H_7) and their cross-linked counterpart x-PE-$NR_3^+Cl^-$.[175] They can be prepared by metallocene-mediated copolymerization of ethylene and reactive comonomers, with and without styrene cross-linkers, respectively (section 3.3).

Table 2 summarizes physical properties of two sets of PE-$NR_3^+Cl^-$ and x-PE-$NR_3^+Cl^-$ membranes (thickness of 50−70 μm) containing high concentrations (25−28 mol %) of pendant $-(CH_2)_4-NR_3^+Cl^-$ groups. For comparison, several commercially available Cl^- ion conductive membranes were also evaluated side-by-side. They include four Neosepta type AEMs produced by Tokuyama Soda and a Selemion high temperature AEM produced by Asahi Glass. They are based on cross-linked styrene/divinylbenzene copolymers with various concentrations of quaternary ammonium chloride groups and cross-linking densities, with or without supporting materials. However, their detailed structural compositions are not available. All Neosepta type commercial membranes have relatively low ion exchange capacities (IEC value between 1 and 2 mmol/g) and low degree of water swelling (DS value below 30%). On the other hand, our PE-$NR_3^+Cl^-$ and x-PE-$NR_3^+Cl^-$

dx.doi.org/10.1021/ma401244t | Macromolecules 2013, 46, 6671−6698

Table 2. Summary of Physical Properties of PE-$NR_3^+Cl^-$, x-PE-$NR_3^+Cl^-$, and Several Commercial Anion-Conductive Membranes

	polymer composition					ionic conductivity (mS/cm)	
samples	ethylene/$-NR_3^+Cl^-$/BSt (mole ratio)	R group	IEC[a] (mmol/g)	DS[b] (%)	λ[c] value	2 N HCl	2 N HCl−0.2 N CuCl
F-1	74.6/25.4/0	H	4.0	126	17.5	30.1	3.6
F-2	74.6/25.4/0	CH_3	3.9	135	19.2	106.1	62.9
F-3	74.6/25.4/0	iso-C_3H_7	3.1	97	17.4	57.6	47.3
G-1	71.7/28.1/0.2	H	3.1	30	5.4	12.4	5.6
G-2	71.7/28.1/0.2	CH_3	2.9	57	10.9	119.6	78.8
G-3	71.7/28.1/0.2	iso-C_3H_7	2.6	45	9.6	27.7	21.1
AHA[d]	no backing material (205 μm)		2.0	22	6.1	12.61	0.66
AMX[d]	with backing fabric (140 μm)		1.5	28	10.4	7.65	2.06
AM-3[d]	highly cross-linked (150 μm)		1.7	20	6.5	4.45	0.25
ACS[d]	monoanion permselective (110 μm)		1.7	25	8.2	5.30	0.22
ACM[d]	cross-linked (100 μm)		1.0	7.5	4.2	4.59	0.005
AHT[e]	high temperature membrane (350 μm)		1.8	10	3.1	4.82	0.11

[a]IEC value is measured by titration. [b]Degree of swelling: g of H_2O/100 g of dry polymer film. [c]Water content λ (molar ratio of water to ammonium chloride). [d]Membrane manufacturers: Tokuyama Soda. [e]Membrane manufacturers: Asahi Glass.

membranes show significantly higher IEC and DS values. Generally speaking, the water swelling in the PE-$NR_3^+Cl^-$ membrane follows with the IEC value. In addition, the degree of hydration per ammonium chloride (λ) increases with the ammonium chloride concentration, indicating a morphological change to become more continuous domains (channels) in PE-$NH_3^+Cl^-$ to ease water swelling. On the other hand, by introducing a very small amount (~0.2 mol %) of BSt cross-linker units in the similar PE copolymer (set G), the water swelling dramatically reduces. In fact, their hydration numbers (λ values) are in the same range of the commercial membranes. In addition, these cross-linked membranes exhibit very good (tough) mechanical strength. The tensile strength at the yield of the G-3 membrane reaches >20 MPa with an elongation at break of 181%,[175] which is more than sufficient to function as an ion conductive membrane in most electrochemical assemblies. It is also interesting to note that the $-N(CH_3)_3^+Cl^-$ group in both non-cross-linked (set F) and cross-linked (set G) membranes shows a higher hydration number than both the $-NH_3^+Cl^-$ and $-N(\text{iso-}C_3H_7)_3^+Cl^-$ groups.

Conductivity of the membrane was measured in 2 N HCl aqueous solution and 2 N HCl−0.2 N CuCl aqueous solution to model the catholyte and anolyte solutions in the CuCl−HCl electrolyzer. All commercial membranes show moderate ionic conductivity (4−13 mS/cm) in 2 N HCl solution and significantly lower conductivity (0.11−2.06 mS/cm) in 2 N HCl−0.2 N CuCl solution. The reduction of Cl^- ion conductivity in 2 N HCl−0.2 N CuCl solution may be due to the association between Cu^+ species and some amino groups in the polymer, thereby reducing the quaternary ammonium chloride (Cl^- carrier) concentration. In fact, during the measurement in 2 N HCl−0.2 N CuCl solution the starting clear solution in the cathode gradually changes to a blue hue in all cases, indicating some type of Cu^{2+} species diffusion throughout the commercial membranes. Most of our PE-$NR_3^+Cl^-$ and x-PE-$NR_3^+Cl^-$ membranes show significantly higher Cl^- ionic conductivity in both 2 N HCl and 2 N HCl−0.2 N CuCl solutions. In each set, they have the same $-NR_3^+Cl^-$ concentration, but a changing R group from H, CH_3, to iso-C_3H_7. It is clear that the conductivity shows strong dependence on R groups, especially in 2 N HCl−0.2 N CuCl solution. Evidently, the bulkier R groups significantly reduce the ionic association between the Cl^- ion and stationery $-NR_3^+$ group, therefore increasing Cl^- ion mobility and the ionic conductivity. The PE-$N(CH_3)_3^+Cl^-$ membrane (F-2) exhibits impressive conductivities of 106.1 mS/cm in 2 N HCl solution and 62.9 mS/cm in 2 N HCl−0.2 N CuCl solution; both are 1 order of magnitude higher than that shown in commercial membranes.[175] However, when the size of the R group is further increasing to the bulkier iso-C_3H_7 group, the IEC value decreases along with its conductivity, due to the dilution effect. A similar trend was also observed in x-PE-$NR_3^+Cl^-$ membranes (set G). As discussed, cross-linking dramatically reduces water swelling and increases ion concentration, which is helpful in ion conductivity. However, cross-linking may also reduce ion mobility. When comparing two parallel sets with a similar $-NR_3^+Cl^-$ (R: H, CH_3, and iso-C_3H_7) concentration, but with or without cross-linking, the conductivity difference is relatively small. In fact, the x-PE-$N(CH_3)_3^+Cl^-$ membrane (G-2) shows slightly higher conductivities of 119.6 mS/cm in 2 N HCl solution and 78.8 mS/cm in 2 N HCl−0.2 N CuCl solution. High mobility of the Cl^- ion in the flexible side chains may minimize the negative ion mobility effect induced by cross-linking. Evidently, the x-PE-$N(CH_3)_3^+Cl^-$ membrane (G-2), containing 28.1 mol % of $C_6N(CH_3)_3^+Cl^-$ units, possesses the structure that results in the best combination of high Cl^- ion concentration and mobility. In addition, the solution in the cathode side remains colorless during the measurement in 2 N HCl−0.2 N CuCl solution, indicating no Cu^{2+} species diffusion through the membrane.

In this study, a new class of high performance polyethylene-based anion exchange membranes has been developed, which contains flexible ammonium chloride ($-NR_3^+Cl^-$) groups and a cross-linking PE network structure. The combination of direct metallocene-mediated copolymerization and effective functional group interconversions in the film form allows us to prepare a wide range of well-defined x-PE-$NR_3^+Cl^-$ membranes with good mechanical strength and relatively low thickness (50−70 μm; without backing material). A systematic structure−property study on both PE-$NR_3^+Cl^-$ and x-PE-$NR_3^+Cl^-$ membranes was performed in order for us to understand the PE structure's effect (concentration of $-NR_3^+Cl^-$ groups, R in the quaternary ammonium group, cross-linking density, etc.) on the water uptake and ionic conductivity. The most desirable x-PE-$NR_3^+Cl^-$ membrane, containing 28.1 mol % $-N(CH_3)_3^+Cl^-$ groups in the flexible side chains, offers an

dx.doi.org/10.1021/ma401244t | Macromolecules 2013, 46, 6671−6698

Scheme 15. Synthesis of PE-*g*-s-PAES Graft Copolymer and Proton Exchange Membrane

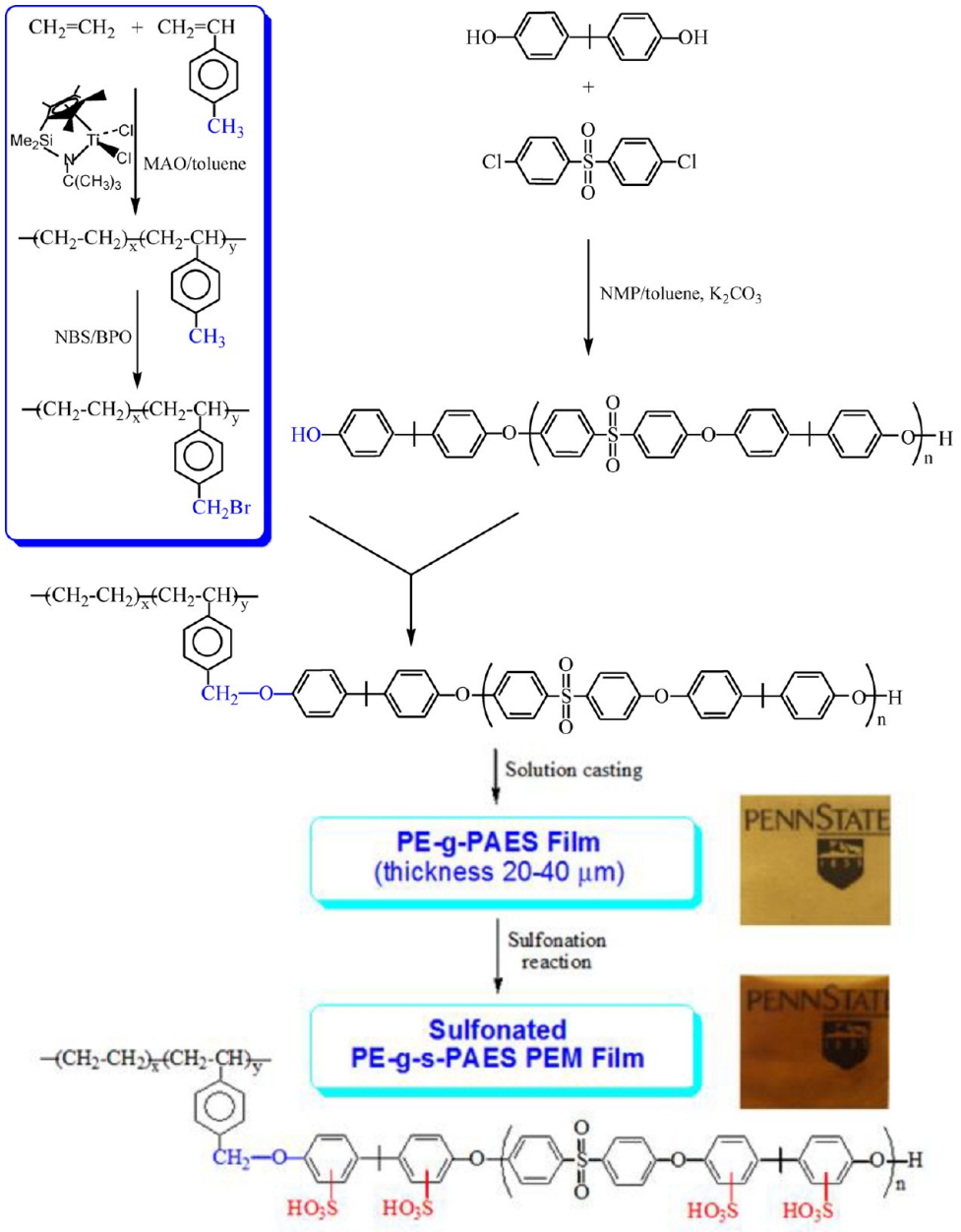

excellent combination of desirable properties, including adequate water swelling, high thermal stability, and exceptionally high ionic conductivities of 119.6 mS/cm in 2 N HCl solution and 78.8 mS/cm in 2 N HCl−0.2 N CuCl solution (1 order higher than commercially available AEM membranes).[175]

Polyethylene Graft Copolymers for Proton Exchange Membranes. We have also applied the polyolefin functionalization chemistry to prepare cationic exchange membranes (CEMs). One example is a PE-*g*-s-PAES graft copolymer containing a high molecular weight PE backbone and several highly sulfonated poly(arylene ethersulfone) (s-PAES) side chains, which is used to prepare proton exchange membranes (PEMs).[176] Scheme 15 illustrates the synthesis route that involves a graft-onto reaction between poly(ethylene-*co*-*p*-bromomethylstyrene) (PE-*co*-*p*-MS-Br) and poly(arylene ether sulfone) (PAES). Both precursor polymers have well-defined molecular structures with molecular weight distribution ($M_w/M_n \sim 2$). The synthesis of PE-*co*-*p*-MS-Br involves a metallocene-mediated ethylene/*p*-MS copolymerization discussed in section 3.3, and the resulting PE-*co*-*p*-MS copolymer was selectively brominated by *N*-bromosuccinimide (NBS). The graft-onto reaction between PE-*co*-*p*-MS-Br and PAES polymers was carried out under the similar condensation polymerization condition used in the preparation of PAES polymers,[177,178] except applying a common anisole solvent for both polymers to maintain a homogeneous condition throughout the coupling reaction. After the coupling reaction, the unreactive PAES polymer was carefully removed by Soxhlet extraction. The resulting PE-*g*-PAES graft copolymer was dissolved in anisole to form a homogeneous and viscous polymer solution before casting into films and then dried to form uniform membranes with thicknesses of 20−40 μm. The formed light brown transparent and ductile membranes were suspended in 1,1,2,2-tetrachloroethane solution for carrying out

dx.doi.org/10.1021/ma401244t | *Macromolecules* 2013, 46, 6671−6698

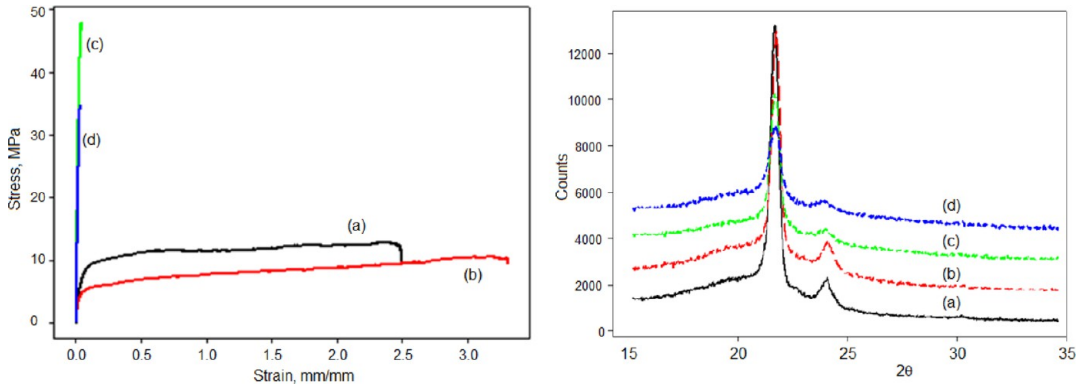

Figure 11. Comparison of strain−stress curves (left) and WAXS patterns (right) for a set of (a) PE-*co*-*p*-MS copolymer (with 1.5 mol % of *p*-MS units; M_v = 390K g/mol), (b) PE-*co*-*p*-MS-Br copolymer (with 0.8 mol % of Br units), (c) the corresponding PE-*g*-PAES graft copolymer containing 63 wt % of PAES, and (d) the corresponding PE-*g*-s-PAES graft copolymer. Reproduced with permission from ref 176.

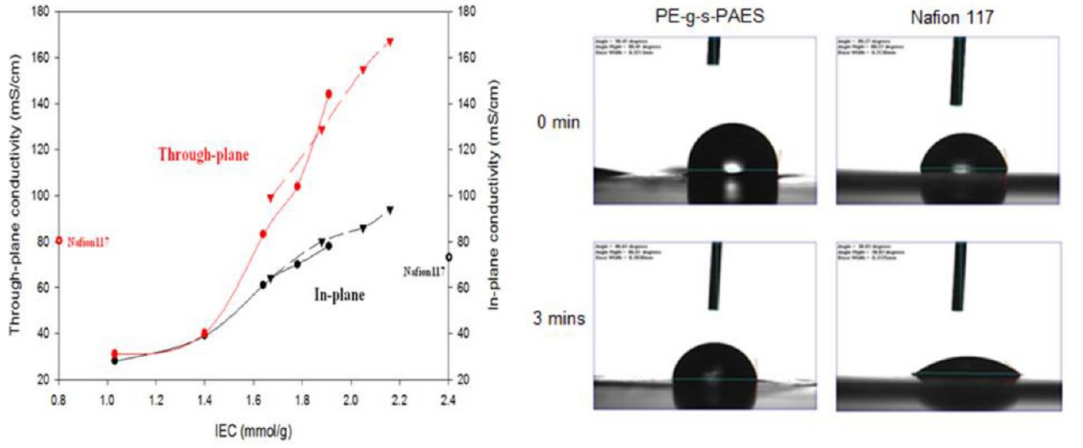

Figure 12. (left) Comparison of in-plane and through-plane conductivities vs IEC values for two sets of PE-s-PAES PEMs (with PE M_v = 390K and 220K g/mol, respectively) and Nafion 117. (right) Comparison of water drop on PE-*g*-s-PAES and Nafion 117. Reproduced with permission from ref 176.

the sulfonation reaction using a trimethylsilyl chlorosulfonate reagent under a heterogeneous condition. The resulting sulfonated PE-*g*-s-PAES films gradually deepened in color, maintaining their transparency and mechanical strength.

Figure 11 (left) compares strain−stress curves of a set of polymers that are formed during the preparation of PE-*g*-s-PAES PEM. The graft copolymers containing PAES (or s-PAES) side chains exhibit very different mechanical profiles than the starting PE-*co*-*p*-MS and PE-*co*-*p*-MS-Br copolymers, which behave like a typical PE thermoplastic with a yield curve showing relatively low tensile strength, low modulus, and high elongation. The high-T_g PAES in the PE-*g*-PAES graft copolymer abruptly increases tensile strength and modulus and decreases the elongation, resembling a high performance engineering plastic. The sulfonated PE-*g*-s-PAES PEM film absorbs some water molecules and still maintains very good mechanical strength with high tensile strength (~35 MPa) and Young's modulus (10 times that of Nafion 117).[176] These mechanical results strongly imply a morphology with many continuous PAES domains imbedded in a highly crystalline PE matrix. Both DSC and WAXS measurements on PE-*g*-s-PAES PEMs reveal the PE crystalline phase. Despite the incorporation of high molecular weight s-PAES side chains, the PE-*g*-s-PAES graft copolymer shows only a small decrease in PE melting temperature and heat of fusion (ΔH). In addition, the PE-*g*-s-PAES graft copolymer also exhibits a T_g at >180 °C, corresponding to the T_g of s-PAES homopolymer. Figure 11 (right) compares the WAXS patterns of the same set of PE copolymers. All samples exhibit two principal PE crystalline diffraction peaks at 2θ = 21.6° and 24.0°, corresponding to the 110 and 200 planes,[179] respectively, with the amorphous halo centered at 2θ = 19.8°. The quantitative determination of the degree of crystallinity (X_c) was estimated by Mandelkern's method,[179] based on an area ratio between crystalline (110 and 200) peaks and the sum of crystalline peaks and amorphous halo. Within the experimental error, there is close agreement between the DSC and WAXS results, indicating only a small change in heat of fusion. Evidently, the PE crystalline phase remains intact during the grafting and sulfonation reactions. All experimental results are consistent with microphase-separated morphology in PE-*g*-s-PAES PEM, with the continuous s-PAES hydrophilic domains (channels) imbedded in a highly crystalline and hydrophobic PE matrix. The hydrophobic and crystalline PE backbone provides a stable (robotic) matrix and enables the sulfonated PAES (s-PAES) side chains in forming highly hydrophilic (acidic) ion-conductive channels across the PEM film.

Most PE-*g*-PAES graft copolymers achieved a higher degree of sulfonation with IEC value ~3.5 mmol/g of s-PAES, corresponding to 1.6−1.7 sulfonic acid per arylene ethersulfone

dx.doi.org/10.1021/ma401244t | *Macromolecules* 2013, 46, 6671−6698

unit in this postsulfonation reaction, despite the heterogeneous reaction condition. It is interesting to note that the sulfonation level reported in the poly(arylene ethersulfone), including the commercial ones,[180−182] was usually less than 1 sulfonic acid per arylene ether sulfone unit. The higher sulfonation level leads to extensive swelling or dissolution by water and polar solvents.[183] It is rather unexpected to see strong PE-*g*-s-PAES PEMs and such a big effect on the water uptake and hydration number (λ) by the PE backbone molecular weight, even in such a high molecular weight range (390K vs 220K g/mol). Comparing similar IEC values (~3.5 mmol/g of s-PAES), the graft copolymers with a 390K g/mol PE backbone show less than half the overall water swelling than that seen in the corresponding graft copolymers with a 220K g/mol PE backbone. Evidently, the water pressure in the PE-*g*-s-PAES with a high IEC value is so high that a PE polymer with extra high molecular weight and crystallinity is needed to contain the water from overswelling. In fact, in a PE-*g*-s-PAES PEM, with PE backbone M_v = 390K g/mol and its IEC value more than double that of Nafion 117, the hydration number for each acid (λ = 14) in PE-*g*-s-PAES is nearly the same as that of Nafion 117 (λ = 15).[176]

Figure 12 (left) compares in-plane and through-plane conductivities for the same two sets of PE-*g*-s-PAES PEMs (with PE backbone M_v = 390K g/mol and 220K g/mol, respectively) and Nafion 117. The conductivity, in essence, proportionately increases with the IEC value. The PE molecular weight appears to be not particularly sensitive to the conductivity. However, good control of water swelling in PE-*g*-s-PAES, with higher PE molecular weight, allows the preparation of PEMs with higher IEC values while still maintaining high mechanical strength. Therefore, the PEMs in the high molecular weight set can reach very high proton conductivity. After the IEC value reaches 1.4, both in-plane and through-plane conductivities accelerate with higher slopes. This turning point implies that the morphology in PE-*g*-s-PAES changes from not fully connected ionic domains to a complete network structure with many ionic channels across the PEM film. In fact, this PEM sample was originated from the PE-*g*-PAES graft copolymer that contains 33 vol % of PAES, which is consistent with the expected percolation threshold.[184−186] It is a pleasant surprise to observe the through-plane conductivity of a PE-*g*-s-PAES PEM reaching 167 mS/cm (double that of Nafion 117) and significantly higher through-plane conductivity than in-plane conductivity in all PE-*g*-s-PAES graft copolymers with percolated ionic channels (IEC value >1.4), which is quite opposite to many reported PEMs.[187−189] The difference becomes larger as the IEC increases. All results indicate a significantly improved connectivity between ion channels, especially in the through-plane direction. Since the through-plane conductivity is directly relative to the fuel cell performance, this is a positive surprise, and it deserved a further study to understand the structure causing this anisotropy in conductivity.

Figure 12 (right) shows the photographs of a water drop on the membrane surface (vs time) for both PE-*g*-s-PAES and Nafion 117 PEMs. When the water drop came in contact with the Nafion 117 PEM surface, the water drop immediately diffused into the matrix. After 3 min, the water drop nearly disappeared from the surface. On the other hand, the PE-*g*-s-PAES PEM retains the water drop very well and only allows the water drop to slowly diffuse into the matrix. Evidently, the surface of PE-*g*-s-PAES is significantly more hydrophobic than the Nafion 117 surface. It is interesting to note that the PE-*g*-s-PAES graft copolymers, possessing even high PAES contents, did not show a contact angle below 90°, which is significantly higher than the 84° of pure poly(arylene ether sulfone). It clearly indicates the preference of PE chains on the PE-*g*-PAES PEM surfaces.[190,191] The corresponding PE-*g*-s-PAES, with a high sulfonic acid concentration, only slightly decreases the contact angle to 98°. The contact angle slowly decreases to 87° after 3 min; the rate of water diffusion through the surface layer of PE-*g*-s-PAES PEM is very slow. The thin PE layer mildly affects in-plane conductivity, but not through-plane conductivity that is essential to the geometry of membrane electrode assembly.

It is also worth noting that in our recent study we have applied PE-*g*-s-PAES PEM in direct methanol fuel cells (DMFCs). We speculate that the existence of a thin hydrophobic (semicrystalline) PE layer on the PEM surface may also offer the barrier property that shall prevent methanol (fuel) crossover from anode to cathode in the direct methanol fuel cells. Methanol fuel loss is a major issue in DMFCs, which leads to lower efficiency and requires thicker PEM membranes. Methanol permeability was measured by monitoring the change of concentration of the water chamber through diffusion of methanol in the methanol solution chamber. We compared, side-by-side, the through-plane methanol permeability and proton conductivity between PE-s-PAES PEM and Nafion 117. Despite much higher IEC values, all PE-s-PAES PEMs show significantly low methanol permeability. A PE-s-PAES PEM shows higher through-plane conductivity; however, the methanol permeability is only one-seventh that of Nafion 117. Its selectivity is more than 7 times higher than that of Nafion 117.

Future Perspectives in Polyolefin-Based Ion Conductors. A new class of PE-based ion conductors (both AEMs and CEMs) has been systematically synthesized and studied to observe several interesting structure and property features. The combination of high molecular weight, crystallinity, cross-linking, and hydrophobicity of the PE backbone is essential to providing a stable matrix (separator function) in the polymer membranes, which allows for the incorporation of a high concentration of ion moieties (exceptionally high IEC values) to form the continuous conductive domains (channels) for performing the ion conduction function, without causing excessive matrix swelling and ion concentration dilution. The *in situ* formed hydrophobic PE molecular layer on the membrane surfaces is advantageous in ion and fuel selectivities and in anisotropic ion conductivity. In addition, the ionic moieties, having flexible methylene spacers from the polymer backbone, in the PE-$NR_3^+Cl^-$ and x-PE-$NR_3^+Cl^-$ membranes seem to point to a unique local molecular structure for ions to achieve high ion mobility and conductivity.

With the availability of functionalization chemistry, new ion-containing polyolefin-based membranes with a broad range of ion moieties, contents, microstructures, and morphologies can be designed and synthesized to offer a set of desirable properties, such as conductivity, water uptake, mechanical strength, selectivity, and also cost-effectiveness. It would be interesting to see polyolefin separators becoming polyolefin polyelectrolytes that could offer higher conductivity (>10^{-3} S/cm) in the solvent-free Li ion batteries under ambient temperatures. In a larger picture, ion exchange membranes and solid polyelectrolytes play essential roles in many electrochemical applications,[133−139] such as the purification of

Scheme 16. Oil-SAP (II) Cycle, Including Synthesis from α-Olefins (I), Absorption of Crude Oil To Form the Corresponding Oil-Absorbed Gel (III), and Thermal Depolymerization Back to α-Olefins (I) and Hydrocarbon Molecules

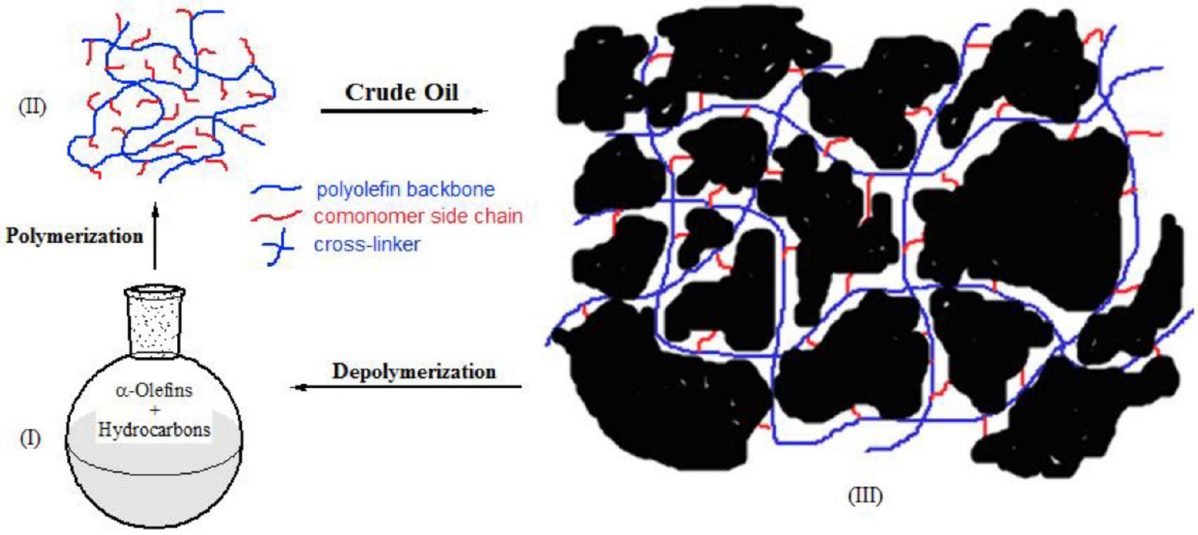

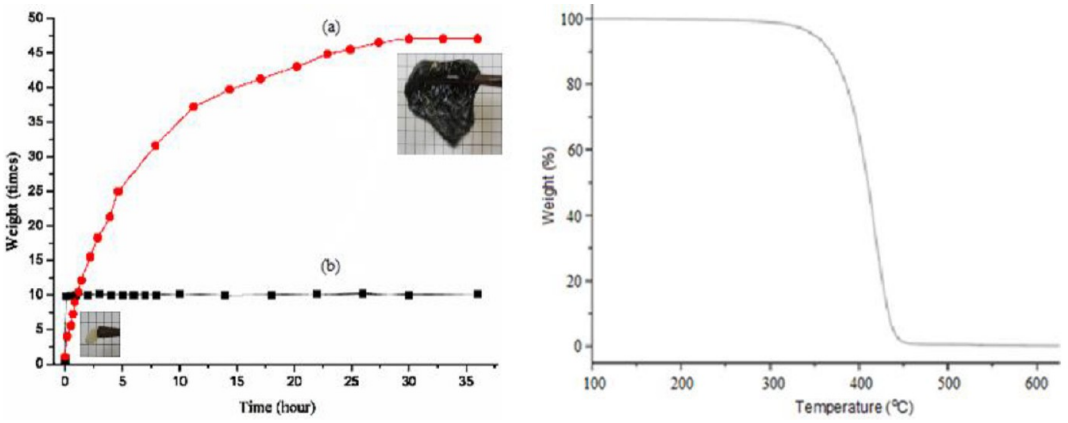

Figure 13. (left) Comparison of oil uptake vs time for (a) cross-linked OS-DVB sample (run A-1) and (b) commercial PP pad; (right) TGA thermograph of cross-linked OS-DVB sample (run A-1) under nitrogen atmosphere. Reproduced with permission from ref 196.

pharmaceuticals, production of salt from seawater, wastewater treatment, and electrochemical devices (i.e., fuel cells, batteries, electrodialysis, electrolysis, electrodeionization, etc.).

4.3. Oil Superabsorbent Polymer for Oil Spill Recovery. As discussed in section 2.4, the challenge to mitigating the environmental impacts from mega oil spills is to find a suitable oil superabsorbent polymer (oil-SAP) that can be quickly and precisely applied on top of an oil spilled site, and the resulting oil-absorbed solid waste can be properly treated without causing secondary pollution. Currently, there are many known superabsorbent polymers (SAP) that are hydrophilic polymers called "hydrogels"[192−195] for absorbing aqueous solutions with enormous absorption capacities, more than 1000 times the polymer weight. In addition to their strong water affinity, they are usually amorphous polymers with a lightly cross-linked network that allows for large volume expansion (water swelling) without dissolution in water. Therefore, the challenge lies in how to design and synthesize analogous oil-SAP polymer (we named it "Petrogel"). It is logical to think of an amorphous polyolefin network structure that contains aliphatic and aromatic monomer units, similar to the hydrocarbon mixtures in crude oils. Since polyolefins are petroleum downstream products, they naturally have a strong physical affinity and similar solubility parameters with hydrocarbon molecules in crude oil. It would be ideal that the recovered oil-SAP solid containing a majority of crude oil could then be directly refined as regular crude oils. Thus, the polyolefin network could be thermally decomposed back to liquid monomers or hydrocarbon molecules. The process would potentially eliminate concerns surrounding how we treat the recovered solid waste while also conserving this precious natural resource. Fortunately, advancement in polyolefin chemistry has allowed us to design and synthesize new polyolefin copolymers with the specific molecular structure and morphology geared toward oil absorption. Scheme 16 shows a schematic presentation of a newly developed oil-SAP "Petrogel" technology[196] and how it works in the synthesis, oil absorption, and recovery/reuse cycle.

One example is an amorphous 1-octene/styrene/divinylbenzene (OS-DVB) terpolymer network (II). The terpolymers, containing various mole ratio of aliphatic and aromatic hydrocarbon monomers and a small DVB (cross-linker) concentration (<2 mol %), were systematically synthesized using metallocene catalyst to form high molecular weight polymers with a broad range of composition, narrow molecular weight and composition distributions, and only engaging

dx.doi.org/10.1021/ma401244t | Macromolecules 2013, 46, 6671−6698

monoenchainment for divinylbenzene (DVB). As discussed in section 3.3, the resulting OS-DVB terpolymer is completely processable in forming various products. However, upon thermal heating (>220 °C) it becomes a completely insoluble network. Seemingly, the oil absorbency and swelling capacity are largely controlled by cross-linking density, inversely proportional to the cross-linking density. There is a minor dependence on the absorbates—either the aliphatic or aromatic hydrocarbons (C_6−C_{12}) or even the mixed oil products.

Figure 13 (left) shows the side-by-side comparison of the oil absorption performance between the cross-linked OS-DVB sample (with 82.3/17.4/0.3 1-octene/styrene/DVB mol %) and a state-of-the-art meltblown PP pad, with a crude containing approximately 70% volatile light oils and 30% nonvolatile heavy oils. The meltblown PP pad is fabricated from a nonwoven fibrous PP textile with a highly crystalline polymer structure and porous morphology (high surface area), which show rapid oil adsorption in their interstices by capillary action, saturating at 10 times the weight of uptake without any visible volume enlargement. The adsorption mechanism happens only on the PP fiber surfaces (not inside the crystalline matrix), which is advantageous with fast kinetics but with limited capacity, and the weak oil−PP interaction results in some adsorbed oil rebleeding under a slight external force. On the other hand, the lightly cross-linked OS-DVB sample (botom picture), with amorphous morphology, gradually absorbs oil in its matrix, increasing its weight by more than 10 times within 10 min and reaching 40 times its weight after 12 h. Its oil sorption capacity is >4 times that of the state-of-the-art meltblown PP pad. As shown in the top image, the resulting oil/oil-SAP mixture can be picked up with a tweezer without leaking oil. In addition, the resulting oil-swelled gel mixture can be treated as crude oil, suitable for regular refining processes. The mixtures contain no water and have nearly the same composition as original crude oil. Figure 13 (right) shows TGA curve of the same lightly cross-linked OS-DVB sample. Under an inert atmosphere, the OS-DVB terpolymer begins its thermal decomposition at 300 °C and rapidly decreases in weight around 400 °C. At 450 °C, the OS-DVB terpolymer was completely decomposed without any residue, indicating the formation of volatile small hydrocarbon molecules. Based on the mass spectrum, the main volatile components are the 1-octene and styrene monomers, with their derivatives having the molecular size below C_{20}. The bulky side chains in 1-octene and styrenic monomer units weaken the C−C bonds along the backbone, which may result in chain scission and the subsequent free radical mediated depolymerization at a relatively low pyrolysis temperature. It is interesting to note that the DVB cross-linking may engage in reversible cyclo-addition during the thermal process (>300 °C). Therefore, the resulting cross-linking structure appears to have little effect on the overall thermal degradation. In other words, during refinery the minor component (2−3%) of OS-DVB polymer will be thermally decomposed back to $<C_{20}$ hydrocarbon molecules (typically existing in crude oil) without residue, well below the typical crude oil refining temperature (>600 °C). This process has multifarious benefits: it eliminates the concern surrounding solid waste disposal, recyclability, and biodegradability, while maintaining our reservations of natural resources. Furthermore, polyolefin products are the most inexpensive of polymeric materials and are capable of large-scale production around the globe.

Overall, the advance in polyolefin chemistry allows us to design and synthesized polyolefin-based oil-SAP materials. The combination of oleophilic and hydrophobic properties with amorphous morphology, high free volume, and a cross-linked network offers a desirable matrix for oil absorption and swelling. The oil uptake is inversely proportional to the cross-linking density. Oil uptake with up to 45 times that of the polymer weight and fast kinetics has been observed in a lightly cross-linked OS-DVB terpolymer. This new oil-SAP technology[196] exhibits a combination of benefits in oil recovery and cleanup, including (i) high oil absorption capability, (ii) fast kinetics, (iii) easy recovery from the water surface, (iv) no water absorption, (v) no waste in natural resources, and (vi) is cost-effective and economically feasible. This new oil-SAP technology shall fundamentally address the multiple issues created by mega oil spills, whether seen from an environmental or economic standpoint.

Future Perspectives in Polyolefin Oil-SAP. Oil spills occur more often than the few highly publicized incidents seen in United States. The reality is that every few years there is a major oil spill due to storage tanks and pipes cracking, oil tanker collisions or wrecks, and even warfare, with deliveries destroying oil facilities. Furthermore, small-scale oil spills are daily occurrences in various facilities, such as gas handling stations, machine shops, and manufacturing facilities. These incidents pollute our underground water, streams, and waterways, silently damaging human health and wildlife. The success of this oil-SAP technology has the potential to fundamentally address issues related to small (daily) or mega (occasionally) oil spills, whether environmental or economic-related. To further increase the effectiveness and efficiency, we are developing the polyolefin oil-SAP with the form that can be applied by low-flying airplanes or helicopters. This new material not only dramatically reduces the responding time to stabilize the spilled oil from dispersion and evaporation under most weather conditions but also reaches the remote locations in a short window of time. It is our primary goal for these new oil-SAP materials to be available in preparation for the next mega oil spill disaster and to be effective in preventing another painful environmental and economic tragedy. Currently, we are also expanding the oil-SAP technology into natural gas storage and separation areas to accommodate the mass adoption of natural gas for transportation.

Overall, we have expanded the superabsorbent polymer (SAP) technology from traditional hydrophilic polymers "Hydrogels" for absorbing aqueous solutions to hydrophobic polymers "Petrogel" for absorbing hydrocarbon solutions. The entire spectrum of experimental results offers the opportunity to systematically compare and understand the key structural features (i.e., composition, microstructure, and morphology) affecting their binding energy, swelling behavior, absorption−desorption kinetics, and the nature of absorbates. In many senses, Petrogel operates in a similar manner to the Hydrogel by providing a good binding energy to absorbate molecules with a swellable network to allow absorbate molecules to diffuse into the polymer matrix and expand the polymer volume. Considering the commercial importance of Hydrogel in our day-to-day life, its applications have been continuously expanding in the past two decades, from disposable sanitary napkins to tissue engineering, cell culture, drug delivery, breast implants, contact lenses, biosensors, soil moisture, etc. It is logical to think that Petrogel could expand its absorption capability to various hydrocarbons (gases, liquids, viscous

matters), which may also include storage, separation, or control release purposes. Some of the applications may only be realized in the future after the prolonged study of this technology.

5. SUMMARY

Polyolefin (PE, PP, etc.) is the material of choice in a broad range of applications, not only in commodities but also in specialties. The lack of chemical functionality and structural diversity are the common barriers for broadening its applications, especially in the specialty areas that require the material to exhibit multiple properties and performance functions. In this paper, I have discussed a powerful functionalization method that can prepare functional polyolefins with well-designed molecular structures. The chemistry is centered in a combination of reactive comonomers and chain transfer agents and metallocene catalysis, having a well-defined and designed single active site, for effective copolymerization and chain transfer reactions. The incorporated reactive sites in polyolefins can be quantitatively interconverted into the desirable functional (polar) groups, "living" macroinitiators, coupling agents for connecting with functional polymer segments. A broad range of functional polyolefins have been prepared with high molecular weight, various functional groups (including cross-linkers), and functional group locations in the side chains, chain ends, and block/graft microstructures. On the other hand, the shape difference in surface energy between polyolefin and functional groups in functional polyolefins results in a unique morphology with clear hydrophobic/hydrophilic microphase separation and a molecular layer of hydrophobic polyolefin on the surfaces. Usually, polyolefin chains, with high hydrophobicity, crystallinity, and melting temperature (if needed, a 3-D network structure), create a stable and strong continuous matrix that allows the hydrophilic functional (polar) groups to form a well-defined second phase with uniform sphere, channel, layer microstructures controlled by volume fraction. The combination of a desirable functional group concentration and well-defined morphology provides the specific functional properties, such as polarizability, conductivity, selectivity, etc., which are beneficial in high-value applications. In this paper, three energy-related applications, including polymer film capacitors for electric energy, ion exchange membranes for hydrogen energy, and oil-SAP for oil spill recovery, have been discussed to show the effects of new functional polyolefin structures on their performances, with the hope of providing inspiration to researchers who may be exploring their new applications.

AUTHOR INFORMATION

Corresponding Author

*E-mail chung@matse.psu.edu.

Notes

The authors declare no competing financial interest.

Biography

Mike Chung received his BS degree in Chemistry from Chung Yuan University (Taiwan) in 1976. He came to the U.S. for his graduate study in the Department of Chemistry, University of Pennsylvania, in 1979. After finishing his Ph.D work in 1982 on conducting polymers (with Professor A. J. MacDiarmid, late Nobel Laureate), he spent two years as a Research Scientist at Institute for polymers and Organic Solids (with Professor Alan J. Heeger, Nobel Laureate), University of California, Santa Barbara. Between 1984 and 1989, he was a Senior Research Staff in Corporate Research, Exxon Company. In 1989, he joined the faculty of the Pennsylvania State University as an associate professor and became professor of Polymer Science in the Department of Materials Science and Engineering in 1993. Professor Chung is interested in the development of new polymer chemistry that can lead to new materials with unique chemical and physical properties. One major theme of his current research is the development of new materials that enable "green" and "sustainable" energy technology. He is author of more than 240 papers, including 55 US and international patents.

ACKNOWLEDGMENTS

The author gratefully acknowledges the financial support of this work through a Multidisciplinary University Research Initiative (MURI) grant from the Office of Naval Research under Contract No. N00014-10-1-0944.

REFERENCES

(1) Natta, G.; Mazzanti, G.; Longi, P.; Bernardini, F. *J. Polym. Sci.* **1958**, *31*, 81.
(2) Boor, J., Jr. *Ziegler-Natta Catalysts and Polymerizations*; Academic Press: London, 1979.
(3) Chung, T. C. *Functionalization of Polyolefins*; Academic Press: London, 2002.
(4) Sinn, H.; Kaminisky, W. *Adv. Organomet. Chem.* **1980**, *18*, 99.
(5) Wild, F. R. W. P.; Zsolnai, L.; Huttner, G.; Brintzinger, H. H. *J. Organomet. Chem.* **1982**, *232*, 233.
(6) Ewen, J. A. *J. Am. Chem. Soc.* **1984**, *106*, 6355.
(7) Kaminsky, W.; Kulper, K.; Brintzinger, H. H.; Wild, F. R. W. P. *Angew. Chem., Int. Ed. Engl.* **1985**, *24*, 507.
(8) Kiesewetter, E. T.; Randoll, S.; Radlauer, M.; Waymouth, R. M. *J. Am. Chem. Soc.* **2010**, *132*, 5566.
(9) Chinsirikul, W.; Chung, T. C.; Harrison, I. *J. Thermoplast. Compos. Mater.* **1993**, *6*, 18.
(10) Lee, S. H.; Li, C. L.; Chung, T. C. *Polymer* **1994**, *35*, 2979.
(11) Chung, T. C.; Lee, S. H. *J. Appl. Polym. Sci.* **1997**, *64*, 567.
(12) Wang, Z. M.; Nakajima, H.; Manias, E.; Chung, T. C. *Macromolecules* **2003**, *36*, 8919.
(13) Winter, M.; Brodd, R. J. *Chem. Rev.* **2004**, *104*, 4245.

(14) Sarjeant, W. J. *Advanced Power Sources for Space Missions, NAS-NRC (EEB) Committee on Advanced Spaced Based High Power Technologies*; National Academy Press: Washington, DC, 1989.
(15) Sarjeant, W.; Zirnheld, J. J.; MacDougall, F. W. *IEEE Trans. Plasma Sci.* **1998**, *26*, 1368.
(16) Reed, C. W.; Cichanowski, S. W. *IEEE Trans. Dielectr. Electr. Insul.* **1994**, *1*, 904.
(17) Sarjeant, W. J.; MacDougall, F. W.; Larson, D. W. *IEEE Electr. Insul. Mag.* **1997**, *13*, 20.
(18) Rabuffi, M.; Picci, G. *IEEE Trans. Plasma Sci.* **2002**, *30*, 1939.
(19) Picci, G.; Rabuffi, M. *IEEE Trans. Plasma Sci.* **2000**, *28*, 1603.
(20) Linden, D.; Reddy, T. B. *Handbook of Batteries*, 3rd ed.; McGraw-Hill: New York, 2002.
(21) Arora, P.; Zhang, Z. *Chem. Rev.* **2004**, *104*, 4419.
(22) Arbatan, T.; Fang, X.; Shen, W. *Chem. Eng. J.* **2011**, *166*, 787.
(23) Karakasi, O. K.; Moutsatsou, A. *Fuel* **2010**, *89*, 3963.
(24) Chol, H. M.; Cloud, R. M. *Environ. Sci. Technol.* **1992**, *26*, 772.
(25) Teas, C.; Kalligeros, S.; Zanikos, F.; Stournas, S.; Lois, E.; Anastopoulos, G. *Desalination* **2001**, *140*, 259.
(26) Inagaki, M.; Kawahara, A.; Konno, H. *Carbon* **2002**, *40*, 105.
(27) Adebajo, M. O.; Frost, R. L.; Kloprogge, J. T.; Carmody, O.; Kokot, S. *J. Porous Mater.* **2003**, *10*, 159.
(28) Deschamps, G.; Caruel, H.; Borredon, M. E.; Bonnin, C.; Vignoles, C. *Environ. Sci. Technol.* **2003**, *37*, 1013.
(29) Suni, S.; Kosunen, A. L.; Hautala, M.; Pasila, A.; Romantschuk, M. *Mar. Pollut. Bull.* **2004**, *49*, 916.
(30) Sun, X. F.; Sun, R. C.; Sun, J. X. *J. Mater. Sci.* **2003**, *38*, 3915.
(31) Bayat, A.; Aghamiri, S. F.; Moheb, A.; Vakili-Nezhaad, G. R. *Chem. Eng. Technol.* **2005**, *28*, 1525.
(32) Wei, Q. F.; Mather, R. R.; Fotheringham, A. F.; Yang, R. D. *Mar. Pollut. Bull.* **2003**, *46*, 780.
(33) Yuan, J.; Liu, X.; Akbulut, O.; Hu, J.; Suib, S. L.; Kong, J.; Stellacci, F. *Nat. Nanotechnol.* **2008**, *3*, 332.
(34) Korhonen, J.; Kettunen, M.; Ras, R.; Ikkala, O. *ACS Appl. Mater. Interfaces* **2011**, *3*, 1813.
(35) Gui, X. C.; Wei, J. Q.; Wang, K. L.; Cao, A. Y.; Zhu, H. W.; Jia, Y.; Shu, Q. K.; Wu, D. H. *Adv. Mater.* **2010**, *22*, 617.
(36) Heller, J.; Tszen, D. O.; Parkinson, D. B. *J. Polym. Sci.* **1963**, *1*, 125.
(37) Hopkins, E.; Miller, M. L. *Polymer* **1963**, *4*, 75.
(38) Bacskai, R. *J. Polym. Sci.* **1965**, *3*, 2491.
(39) Clark, K. J.; Powell, T. *Polymer* **1965**, *6*, 531.
(40) Purgett, M. D.; Vogl, O. *J. Polym. Sci., Part A: Polym. Chem.* **1988**, *26*, 677.
(41) Kesti, M. R.; Coates, G. W.; Waymouth, R. M. *J. Am. Chem. Soc.* **1992**, *114*, 9679.
(42) Stehling, U. M.; Stein, K. M.; Kesti, M. R.; Waymouth, R. M. *Macromolecules* **1998**, *31*, 2019.
(43) Stehling, U. M.; Stein, K. M.; Fisher, D.; Waymouth, R. M. *Macromolecules* **1999**, *32*, 14.
(44) Schneider, M. J.; Schäfer, R.; Mülhaupt, R. *Polymer* **1996**, *38*, 2455.
(45) Boffa, L. S.; Novak, B. M. *Chem. Rev.* **2000**, *100*, 1479.
(46) Ittel, S. D.; Johnson, L. K.; Brookhart, M. *Chem. Rev.* **2000**, *100*, 1169.
(47) Nakamura, A.; Ito, S.; Nozaki, K. *Chem. Rev.* **2009**, *109*, 5215.
(48) Chen, E. Y. X. *Chem. Rev.* **2009**, *109*, 5157.
(49) Johnson, L. K.; Killian, C. M.; Brookhart, M. *J. Am. Chem. Soc.* **1995**, *117*, 6414.
(50) Johnson, L. K.; Mecking, S.; Brookhart, M. *J. Am. Chem. Soc.* **1996**, *118*, 267.
(51) Mecking, S.; Johnson, L.; Wang, L.; Brookhart, M. *J. Am. Chem. Soc.* **1998**, *120*, 888.
(52) Correia, S. G.; Marques, M. M.; Ascenso, J. R.; Ribeiro, A. F. G.; Gomes, P. T.; Dias, A. R.; Blais, M.; Rausch, M. D.; Chien, J. C. W. *J. Polym. Sci., Part A: Polym. Chem.* **1999**, *37*, 2471.
(53) Luo, S.; Vela, J.; Lief, G. R.; Jordan, R. F. *J. Am. Chem. Soc.* **2007**, *129*, 8946.
(54) Guironnet, D.; Roesle, P.; Runzi, T.; Gottker-Schnetmann, I.; Mecking, S. *J. Am. Chem. Soc.* **2009**, *131*, 422.
(55) Runzi, T.; Frohlich, D.; Mecking, S. *J. Am. Chem. Soc.* **2010**, *132*, 17690.
(56) Ito, S.; Munakata, K.; Nakamura, A.; Nozaki, K. *J. Am. Chem. Soc.* **2009**, *131*, 14606.
(57) Ito, S.; Kanazawa, M.; Munakata, K.; Kuroda, J. I.; Okumura, Y.; Nozaki, K. *J. Am. Chem. Soc.* **2011**, *133*, 1232.
(58) Singh, R. P. *Prog. Polym. Sci.* **1992**, *17*, 251.
(59) Jagur-Grodzinski, J. *Prog. Polym. Sci.* **1992**, *17*, 361.
(60) Trivedi, B. C.; Culbertson, B. M. *Maleic Anhydride*; Plenum Press: New York, 1982.
(61) Gilman, J. W.; Jackson, C. L.; Morgan, A. B.; Harris, R., Jr.; Manias, E.; Giannelis, E. P.; Wuthenow, M.; Hilton, D.; Phillips, S. H. *Chem. Mater.* **2000**, *12*, 1866.
(62) Maiti, P.; Nam, P. H.; Okamoto, M.; Hasegawa, N.; Usuki, A. *Macromolecules* **2002**, *35*, 2042.
(63) Ray, S. S.; Okamato, M. *Prog. Polym. Sci.* **2003**, *28*, 1539.
(64) Lambla, M. *Comprehensive Polymer Science, First Supplement*; Allen, G., Ed.; Pergamon Press: New York, 1982.
(65) Simmons, A.; Baker, W. E. *Polym. Eng. Sci.* **1989**, *29*, 1117.
(66) Coutinho, F. M. B.; Ferfeira, M. I. *Eur. Polym. J.* **1994**, *30*, 911.
(67) Ostenbrink, A. J.; Gaymans, R. J. *Polymer* **1992**, *33*, 3086.
(68) Gaylord, N. G.; Mehta, M. *J. Polym. Sci., Polym. Lett. Ed.* **1982**, *20*, 481.
(69) Heinen, W.; Rosenmoller, C. H.; Wenzel, C. B.; deGroot, H. J. M.; Lugtenburg, J. *Macromolecules* **1996**, *29*, 1151.
(70) Passaglia, E.; Coiai, S.; Augier, S. *Prog. Polym. Sci.* **2009**, *34*, 911.
(71) Chung, T. C. *Prog. Polym. Sci.* **2002**, *27*, 39.
(72) Chung, T. C. *Macromolecules* **1988**, *21*, 865.
(73) Ramakrishnan, S.; Berluche, E.; Chung, T. C. *Macromolecules* **1990**, *23*, 378.
(74) Chung, T. C.; Rhubright, D. *Macromolecules* **1991**, *24*, 970.
(75) Chung, T. C. *Polym. Mater. Encycl.* **1996**, *4*, 2681.
(76) Wang, L.; Wan, D.; Zhang, Z. J.; Liu, F.; Xing, H. P.; Wang, Y. H.; Tang, T. *Macromolecules* **2011**, *44*, 4167.
(77) Wang, L.; Wan, D.; Qiu, J.; Tang, T. *Polymer* **2012**, *53*, 4737.
(78) Chung, T. C.; Rhubright, D. *Macromolecules* **1994**, *27*, 1313.
(79) Lu, B.; Chung, T. C. *Macromolecules* **1999**, *32*, 2525.
(80) Brown, H. C. *Organic Synthesis via Boranes*; Wiley-Interscience: New York, 1975.
(81) Chung, T. C.; Rhubright, D. *Macromolecules* **1993**, *26*, 3019.
(82) Dong, J. Y.; Manias, E.; Chung, T. C. *Macromolecules* **2002**, *35*, 3439.
(83) Chung, T. C.; Lu, H. L.; Li, C. L. *Polym. Int.* **1995**, *37*, 197.
(84) Chung, T. C.; Lu, H. L. *J. Polym. Sci., Polym. Chem. Ed.* **1997**, *35*, 575.
(85) Chung, T. C.; Lu, H. L. *J. Polym. Sci., Polym. Chem. Ed.* **1998**, *36*, 1017.
(86) Chung, T. C.; Lu, H. L. *J. Polym. Sci., Polym. Chem. Ed.* **1999**, *37*, 2795.
(87) Chung, T. C.; Hong, S.; Lu, H. L. *Macromolecules* **1998**, *31*, 2028.
(88) Chung, T. C. *J. Elastomers Plast.* **1999**, *31*, 298.
(89) Lu, B.; Chung, T. C. *J. Polym. Sci., Polym. Chem. Ed.* **2000**, *38*, 1337.
(90) Frechet, J. M. J. *Crown Ethers and Phase Transfer Catalysts in Polymer Science*; Plenum Press: New York, 1984.
(91) Powers, K. W.; Wang, H. C.; Chung, T. C.; Jias, A. J.; Olkusz, J. A. US. Patent 5,162,445.
(92) Mohanraj, S.; Ford, W. *Macromolecules* **1986**, *19*, 2470.
(93) Pini, D.; Settambolo, R.; Raffaelli, A.; Salvadori, P. *Macromolecules* **1987**, *20*, 58.
(94) Jones, R. G.; Matsubayashi, Y. *Polymer* **1992**, *33*, 1069.
(95) Nagasaki, Y.; Tsuruta, T. *Makromol. Chem., Rapid Commun.* **1986**, *7*, 437.
(96) Ferrari, L. P.; Stover, H. D. *Macromolecules* **1991**, *24*, 6340.
(97) Zambelli, A.; Pellecchia, C.; Oliva, L.; Longo, P.; Crassi, A. *Makromol. Chem.* **1991**, *192*, 223.

(98) Zambelli, A.; Pellecchia, C.; Proto, A. *Macromol. Symp.* **1995**, *89*, 373.
(99) Longo, P.; Proto, A.; Zambelli, A. *Macromol. Chem. Phys.* **1995**, *196*, 3015.
(100) Zhang, M.; Colby, R. H.; Milner, S. T.; Chung, T. C. *Macromolecules* **2013**, *46*, 4313.
(101) Dong, J. Y.; Chung, T. C. *Macromolecules* **2002**, *35*, 2868.
(102) Dong, J. Y.; Hong, H.; Chung, T. C.; Wang, H. C.; Datta, S. *Macromolecules* **2003**, *36*, 6000.
(103) Lin, W.; Shao, Z.; Dong, J. Y.; Chung, T. C. *Macromolecules* **2009**, *42*, 3750.
(104) Mayo, F. R. *J. Am. Chem. Soc.* **1953**, *75*, 6133.
(105) Hagihara, H.; Tsuchihara, K.; Sugiyama, J.; Takeuchi, K.; Shiono, T. *Macromolecules* **2004**, *37*, 5145.
(106) Hu, Y.; Carlson, E. D.; Fuller, G. G.; Waymouth, R. M. *Macromolecules* **1999**, *32*, 3334.
(107) Xu, G.; Chung, T. C. *J. Am. Chem. Soc.* **1999**, *121*, 6763.
(108) Xu, G.; Chung, T. C. *Macromolecules* **1999**, *32*, 8689.
(109) Chung, T. C.; Xu, G.; Lu, Y. Y.; Hu, Y. *Macromolecules* **2001**, *34*, 8040.
(110) Lin, W.; Dong, J. Y.; Chung, T. C. *Macromolecules* **2008**, *41*, 8452.
(111) Lin, W.; Niu, H.; Chung, T. C.; Dong, J. Y. *J. Polym. Sci., Part A: Polym. Chem.* **2010**, *48*, 3534.
(112) Chung, T. C.; Dong, J. Y. *J. Am. Chem. Soc.* **2001**, *123*, 4871.
(113) Dong, J. Y.; Chung, T. C. *Macromolecules* **2002**, *35*, 1622.
(114) Dong, J. Y.; Wang, Z. M.; Han, H.; Chung, T. C. *Macromolecules* **2002**, *35*, 9352.
(115) Chung, T. C.; Jiang, G. J. *Macromolecules* **1992**, *25*, 4816.
(116) Chung, T. C.; Jiang, G. J.; Rhubright, D. *Macromolecules* **1993**, *26*, 3467.
(117) Chung, T. C.; Janvikul, W.; Bernard, R.; Jiang, G. J. *Macromolecules* **1994**, *27*, 26.
(118) Chung, T. C. *Polym. Mater. Encycl.* **1996**, *8*, 6412.
(119) Chung, T. C.; Lu, H. L.; Ding, R. D. *Macromolecules* **1997**, *30*, 1272.
(120) Lu, H. L.; Chung, T. C. *J. Polym. Sci., Polym. Chem. Ed.* **1999**, *37*, 4176.
(121) Chung, T. C.; Lu, H. L. *J. Mol. Catal. A: Chem.* **1997**, *115*, 115.
(122) Chung, T. C.; Lu, H. L.; Janvikul, W. *Polymer* **1997**, *38*, 1495.
(123) Langston, J.; Dong, J. Y.; Chung, T. C. *Macromolecules* **2005**, *38*, 5849.
(124) Langston, J. A.; Colby, R. H.; Shimizu, F.; Suzuki, T.; Aoki, M.; Chung, T. C. *Macromolecules* **2007**, *40*, 2712.
(125) Gao, C.; Zou, J.; Dong, J. Y.; Hu, Y. L.; Chung, T. C. *J. Polym. Sci., Polym. Chem. Ed.* **2005**, *43*, 429.
(126) Chung, T. C.; Lu, H. L.; Janvikul, W. *J. Am. Chem. Soc.* **1996**, *118*, 705.
(127) Zhang, Z. C.; Chung, T. C. *Macromolecules* **2006**, *39*, 5187.
(128) Wang, Z.; Zhang, Z. C.; Chung, T. C. *Macromolecules* **2006**, *39*, 4268.
(129) Zhang, Z. C.; Chung, T. C. *Macromolecules* **2007**, *40*, 783.
(130) Zhang, Z. C.; Chung, T. C. *Macromolecules* **2007**, *40*, 9391.
(131) Yuan, X.; Matsuyama, Y.; Chung, T. C. *Macromolecules* **2010**, *43*, 4011.
(132) Yuan, X.; Chung, T. C. *Appl. Phys. Lett.* **2011**, *98*, 62901.
(133) Gray, F. M. *Solid Polymer Electrolytes*; VCH: New York, 1991.
(134) *Polymer Electrolyte Reviews*; MacCallum, J. R., Vincent, C. A., Eds.; Elsevier Applied Science: New York, 1987.
(135) Sata, T. *Pure Appl. Chem.* **1986**, *58* (12), 1613.
(136) Rikukawa, M.; Sanui, K. *Prog. Polym. Sci.* **2000**, *25*, 1463.
(137) Brandon, N. P.; Skinner, S.; Steele, B. C. H. *Annu. Rev. Mater. Res.* **2003**, *33*, 183.
(138) Hickner, M. A.; Ghassemi, H.; Kim, Y. S.; Einsla, B. R.; McGrath, G. E. *Chem. Rev.* **2004**, *104*, 4587.
(139) Wang, C.; Chalkova, E.; Lute, C.; Fedkin, M.; Komarneni, S.; Chung, T. C.; Lvov, S. *J. Electrochem. Soc.* **2010**, *157*, 1634.
(140) Robitaille, C. D.; Fauteux, D. *J. Electrochem. Soc.* **1986**, *133*, 315.
(141) Labreche, C.; Levesque, I.; Prud'homme, J. *Macromolecules* **1996**, *29*, 7795.
(142) Edman, L.; Ferry, A.; Doeff, M. M. *J. Mater. Res.* **2000**, *15*, 1950.
(143) Obeidi, Sh.; Stolwijk, N. A. *Macromolecules* **2005**, *38*, 10750.
(144) Fullerton-Shirey, S. K.; Maranas, J. K. *Macromolecules* **2009**, *42*, 2142.
(145) Grot, W. G. E. I. DuPont, US Patent 4,433,082, 1984.
(146) Savadogo, O. *J. New Mater. Electrochem. Syst.* **1998**, *1*, 47.
(147) Gottesfeld, S.; Zawodzinski, T. A. In *Advances in Electrochemical. Science and Engineering*; Alkire, R. C., Gerischer, H., Kolb, D. M., Tobias, C. W., Eds.; Wiley: New York, 2002; Vol. 5.
(148) Wainright, J. S.; Wang, J.-T.; Weng, D.; Savinell, R. F.; Litt, M. *J. Electrochem. Soc.* **1995**, *142*, L121.
(149) Wang, F.; Hickner, M. A.; Ji, Q.; Harrison, W.; Mecham, J.; Zawodzinski, T. A.; McGrath, J. E. J. *Macromol. Symp.* **2001**, *75*, 387.
(150) Wang, J.; Zhao, Z.; Gong, F.; Li, S.; Zhang, S. *Macromolecules* **2009**, *42*, 8711.
(151) Yan, J.; Hickner, M. A. *Macromolecules* **2010**, *43*, 2349.
(152) Wang, J.; Li, S.; Zhang, S. *Macromolecules* **2010**, *43*, 3890.
(153) Tishchenko, G.; Bleha, M.; Skvor, J.; Bures, L.; Mizutani, Y.; Ohmura, N. *J. Appl. Polym. Sci.* **1995**, *58*, 1341.
(154) Wu, H. S.; Wu, Y. K. *Macromolecules* **2005**, *44*, 1757.
(155) Lin, B.; Qiu, L.; Lu, J.; Yan, F. *Chem. Mater.* **2010**, *22*, 6718.
(156) Danks, T. N.; Slade, R. C. T.; Varcoe, J. R. *J. Mater. Chem.* **2002**, *12*, 3371.
(157) Danks, T. N.; Slade, R. C. T.; Varcoe, J. R. *J. Mater. Chem.* **2003**, *13*, 712.
(158) Lee, W.; Saito, K.; Furusaki, S.; Sugo, T.; Makuuchi, K. *J. Membr. Sci.* **1993**, *81*, 295.
(159) Nasefa, M. M.; Hegazy, E. S. A. *Prog. Polym. Sci.* **2004**, *29*, 499.
(160) Varcoe, J. R.; Slade, R. C. *Fuel Cells* **2004**, *4* (4), 1.
(161) Herman, H.; Slade, R. C. T.; Varcoe, J. R. *J. Membr. Sci.* **2003**, *218*, 147.
(162) Lin, M. C.; Takai, N. *J. Membr. Sci.* **1994**, *88*, 77.
(163) Kostov, G. K.; Turmanova, S. C. *J. Appl. Polym. Sci.* **1997**, *64*, 1469.
(164) Kawabe, H.; Yanagita, M. *Bull. Chem. Soc. Jpn.* **1969**, *42*, 1029.
(165) Trochimczuk, W. M. *J. Polym. Sci., Polym. Chem. Ed.* **1975**, *13*, 357.
(166) Kolhe, S. M.; Kumar, A. *Radiat. Phys. Chem.* **2005**, *74*, 384.
(167) Novoselova, L. Y.; Sirotkina, E. E. *Chem. Sustainable Dev.* **2006**, *14*, 199.
(168) Robertson, N. J.; Kostalik, H. A., IV; Clark, T. J.; Mutolo, P. F.; Abruna, H. D.; Coates, G. W. *J. Am. Chem. Soc.* **2010**, *132*, 3400.
(169) Kostalik, H. A., IV; Clark, T. J.; Robertson, N. J.; Mutolo, P. F.; Longo, J. M.; Abruna, H. D.; Coates, G. W. *Macromolecules* **2010**, *43*, 7147.
(170) Noonan, K. J. T.; Hugar, K. M.; Kostalik, H. A., IV; Lobkovsky, E. B.; Abruna, H. D.; Coates, G. W. *J. Am. Chem. Soc.* **2012**, *134*, 18161.
(171) Aitken, B. S.; Lee, M.; Hunley, M. T.; Gibson, H. W.; Wagener, K. B. *Macromolecules* **2010**, *43*, 1699.
(172) Aitken, B. S.; Buitrago, C. F.; Heffley, J. D.; Lee, M.; Gibson, H. W.; Winey, K. I.; Wagener, K. B. *Macromolecules* **2012**, *45*, 681.
(173) Lewis, M. A.; Masin, J. G.; O'Hare, P. A. *Int. J. Hydrogen Energy* **2009**, *34*, 4115.
(174) Balashov, V. N.; Schatz, R.; Chalkova, E.; Akinfiev, N. N.; Fedkin, M. V.; Lvov, S. N. *J. Electrochem. Soc.* **2011**, *158*, B266.
(175) Zhang, M.; Kim, H. K.; Lvov, S. N.; Chung, T. C. *Macromolecules* **2011**, *44*, 5937.
(176) Kim, H. Y.; Zhang, M.; Yuan, X.; Chung, T. C. *Macromolecules* **2012**, *45*, 2460.
(177) Lee, H. S.; Roy, A.; Lane, O.; Dunn, S.; McGrath, J. E. *Polymer* **2008**, *49*, 715.
(178) Kwon, Y. H.; Kim, S. C.; Lee, S. Y. *Macromolecules* **2009**, *42*, 5244.
(179) Gopalan, M. R.; Mandelkern, L. *J. Polym. Sci., Part B: Polym. Lett.* **1967**, *5*, 925.

(180) Baradie, B.; Poinsignon, C.; Sanchez, J. Y.; Piffard, Y.; Vitter, G.; Bestaoui, N.; Foscallo, D.; Denoyelle, A.; Delabouglise, D.; Vaujany, M. *J. Power Sources* **1998**, *74*, 8.
(181) Lufrano, F.; Baglio, V.; Staiti, P.; Arico', A. S.; Antonucci, V. *J. Power Sources* **2008**, *179*, 34.
(182) Nolte, R.; Ledjeff, K.; Bauer, M.; Mülhaupt, R. *J. Membr. Sci.* **1993**, *83*, 211.
(183) Wang, F.; Hickner, M.; Kim, Y. S.; Zawodzinski, T. A.; McGrath, J. E. *J. Membr. Sci.* **2002**, *197*, 231.
(184) Gebel, G. *Polymer* **2000**, *41*, 5829.
(185) Khandpur, A. K.; Foerster, S.; Bates, F. S.; Hamley, I. W.; Ryan, A. J.; Bras, W.; Almdal, K.; Mortensen, K. *Macromolecules* **1995**, *28*, 8796.
(186) Hasegawa, H.; Tanaka, H.; Yamasaki, K.; Hashimoto, T. *Macromolecules* **1987**, *20*, 1651.
(187) Takamuku, S.; Takimoto, N.; Abe, M.; Shinohara, K. *J. Power Sources* **2010**, *195*, 1095.
(188) Soboleva, T.; Xie, Z.; Shi, Z.; Tsang, E.; Navessin, T.; Holdcroft, S. *J. Electroanal. Chem.* **2008**, *622*, 145.
(189) Peckham, T. J.; Holdcroft, S. *Adv. Mater.* **2010**, *22*, 4667.
(190) Gaines, G. L., Jr. *Macromolecules* **1981**, *14*, 208.
(191) Thomas, H. R.; O'Malley, J. J. *Macromolecules* **1979**, *12*, 323.
(192) Gehrke, S. H. *Adv. Polym. Sci.* **1993**, *110*, 81.
(193) Osada, Y.; Gong, J. P. *Adv. Mater.* **1998**, *10*, 827.
(194) Kawaguchi, H. *Prog. Polym. Sci.* **2000**, *25*, 1171.
(195) Park, M. H.; Joo, M. K.; Choi, B. G.; Jeong, B. *Acc. Chem. Res.* **2012**, *45*, 424.
(196) Yuan, X.; Chung, T. C. *Energy Fuels* **2012**, *26*, 4896.